The Journal of Comparative Neurology
Research in Systems Neuroscience
DOI 10.1002/cne.23751

Expression and cellular localization of the voltage-gated calcium channel $\alpha_2\delta_3$ in the rodent retina

Luis Pérez de Sevilla Müller[1], Allison Sargoy[1,2,3], Laura Fernández-Sánchez[6], Allen Rodriguez[1], Janelle Liu[1], Nicolás Cuenca[6] and Nicholas Brecha[1,2,3,4,5]

[1]Departments of [1]Neurobiology and [2]Medicine, [3]Jules Stein Eye Institute, [4]CURE-Digestive Diseases Research Center, David Geffen School of Medicine at UCLA, University of California, Los Angeles, CA 90095; [5]Veterans Administration Greater Los Angeles Healthcare System, Los Angeles, CA 90073; [6]Physiology, Genetics & Microbiology, University of Alicante, Spain.

Key words: calcium channel, retina, $\alpha_2\delta_3$ subunit, amacrine cell, ganglion cell, photoreceptor

Short title: $\alpha_2\delta_3$ subunit in the rodent retina

Editor-in-Chief, Journal of Comparative Neurology

Corresponding author:
Dr. Luis Pérez de Sevilla Müller
Department of Neurobiology
David Geffen School of Medicine at Los Angeles
University of California, Los Angeles
10833 Le Conte Ave.
Los Angeles, California 90095-1763

Email: luisperez@mednet.ucla.edu

Phone: 310-825-6758

Fax: 310-825-2224

Pages: 33

Word count: 10818

Figures: 10

Support or grant information

This research and development project was conducted by David Geffen School of Medicine at UCLA and is made possible by a contract that was awarded and administered by the U.S. Army Medical Research &

Received: Sep 08, 2014; Revised: Jan 21, 2015; Accepted: Jan 24, 2015

Materiel Command (USAMRMC) and the Telemedicine & Advanced Technology Research Center (TATRC), at Fort Detrick, MD under Contract Number: W81XWH-10-2-0077. Support for these studies was also from NIH EY04067 and a VA Merit Review (NB). NCB is a VA Career Research Scientist.

Abstract

High voltage activated calcium channels are hetero-oligomeric protein complexes that mediate multiple cellular processes including the influx of extracellular Ca^{2+}, neurotransmitter release, gene transcription and synaptic plasticity. These channels consist of a primary $\alpha 1$ pore-forming subunit, which is associated with an extracellular $\alpha_2\delta$ subunit and an intracellular β auxiliary subunit, which alter the gating properties and trafficking of the calcium channel. The cellular localization of the $\alpha_2\delta_3$ subunit in the mouse and rat retina is unknown. In this study, using RT-PCR a single band at ~305 bp corresponding to the predicted size of the $\alpha_2\delta_3$ subunit fragment was in mouse and rat retina and brain homogenates. Western blotting of rodent retina and brain homogenates showed a single 123 kDa band. Immunohistochemistry using an affinity purified antibody to the $\alpha_2\delta_3$ subunit revealed immunoreactive cell bodies in the ganglion cell layer (GCL) and inner nuclear layer (INL), and immunoreactive processes in the inner plexiform layer (IPL) and the outer plexiform layer (OPL). $\alpha_2\delta_3$ immunoreactivity was localized to multiple cell types, including ganglion, amacrine and bipolar cells, and photoreceptors, but not by horizontal cells. The expression of the $\alpha_2\delta_3$ calcium channel subunit to multiple cell types suggests this subunit participates widely in Ca channel-mediated signaling in the retina.

Introduction

High voltage activated (HVA) calcium channels are transmembrane proteins comprised of an α1 subunit that contains the channel pore and voltage-sensor, and $\alpha_2\delta$ and β auxiliary subunits (reviewed in Catterall, 2000). The α1 subunits establish the biophysical and pharmacological properties of the calcium channel (Catterall, 2000). The $\alpha_2\delta$ genes (CACNA2D1-4) encode four different $\alpha_2\delta$ subunits, $\alpha_2\delta_1$-$\alpha_2\delta_4$ (Klugbauer et al., 1999). The predominantly, extracellular $\alpha_2\delta$ subunits regulate plasma membrane trafficking and expression of the α1 subunit as well as altering the biophysical properties of the channel (reviewed in Davies et al., 2007; Bauer et al., 2010; Dolphin, 2012).

The $\alpha_2\delta$ subunits are expressed differentially in the brain (Klugbauer et al., 1999; Barclay et al., 2001; Brodbeck et al., 2002; Cole et al., 2005) and retina (Nakajima et al., 2009; Huang et al., 2013; Pérez de Sevilla Müller et al., 2013). $\alpha_2\delta_1$ mRNA is reported in mouse cerebellar, hippocampal and cortical extracts (Klugbauer et al., 1999; Cole et al., 2005). In the central nervous system (CNS), $\alpha_2\delta_1$ subunit immunoreactivity is observed at all levels of the neuroaxis, including the spinal cord, brain stem, thalamus and forebrain (Taylor and Garrido, 2008). In hippocampus, $\alpha_2\delta_1$ subunit immunostaining is heterogeneous with a greater density in areas having glutamate terminals (Taylor and Garrido, 2008). In the rat retina, the majority of ganglion cells, as well as amacrine, bipolar and horizontal cells express the $\alpha_2\delta_1$ subunit (Huang et al., 2013). In addition, Müller cells and astrocytes express the $\alpha_2\delta_1$ subunit (Huang et al., 2013). In the mouse and rat CNS, $\alpha_2\delta_2$ mRNA is strongly expressed in cerebellar Purkinje cells and in interneurons of the cortex, hippocampus and striatum (Barclay et al., 2001; Brodbeck et al., 2002; Cole et al., 2005). There are no reports that we are aware of concerning $\alpha_2\delta_2$ immunoreactivity in the retina. $\alpha_2\delta_3$ mRNA expression was initially reported to be restricted to multiple regions of the mouse CNS (Angelotti and Hofmann, 1996; Klugbauer et al., 1999). A subsequent study however, reported $\alpha_2\delta_3$ mRNA expression in ON bipolar cells of the mouse retina using *in situ* hybridization histochemistry (Nakajima et al., 2009). In addition, $\alpha_2\delta_3$ subunit expression has been detected in rat atria (Chu and Best, 2003) and human heart, skeletal muscle and kidney (Gong et al., 2001). Finally, the gene encoding the $\alpha_2\delta_3$ subunit has been implicated

as a tumor suppressor gene in human gastric cancer cells (Wanajo et al., 2008). The $\alpha_2\delta_4$ subunit is expressed in non-neuronal endocrine cells (Arikkath and Campbell, 2003; Klugbauer et al., 2003). Recently, we reported $\alpha_2\delta_4$ mRNA in mouse and rat CNS and retina; $\alpha_2\delta_4$ subunit immunostaining was present in Müller cells and a few displaced ganglion cells, as well as ON bipolar cell dendritic tips and photoreceptor terminals (Pérez de Sevilla Müller et al., 2013). $\alpha_2\delta_4$ subunit immunoreactivity has also been localized to salamander photoreceptor terminals (Mercer et al., 2011). Interestingly, a mutation in the Cacna2d4 gene has been implicated in a novel cone-rod retinal disease in mouse (Ruether et al., 2000; Wycisk et al., 2006a, b).

The goal of the present study was to establish the expression and cellular localization of the $\alpha_2\delta_3$ subunit in rat and mouse retina. $\alpha_2\delta_3$ mRNA was detected in retina and brain by RT-PCR and a single band corresponding to the predicted size of the $\alpha_2\delta_3$ subunit was detected in retina and brain extracts on Western blots. Cell bodies in the ganglion cell layer (GCL) and inner nuclear layer (INL) contain $\alpha_2\delta_3$ subunit immunoreactivity, and processes in the inner plexiform layer (IPL) and puncta in the outer plexiform layer (OPL) have strong $\alpha_2\delta_3$ subunit immunoreactivity. Double-label immunostaining experiments demonstrated the expression of $\alpha_2\delta_3$ subunit in all retinal cell types except Müller and horizontal cells. These findings suggest that the $\alpha_2\delta_3$ subunit has a broad influence in the retina, and mediates HVA channel properties that would affect intracellular signaling pathways, neurotransmitter release, neuronal excitation, synaptic stabilization and synaptogenesis (Arikkath and Campbell, 2003; Dickman et al., 2008; Eroglu et al., 2009; Kurshan et al., 2009).

Methods and Materials

Animal preparation: All experiments were carried out in accordance with the guidelines for the welfare of experimental animals issued by the U.S. Public Health Service Policy on Human Care and Use of Laboratory Animals and the University of California-Los Angeles (UCLA) Animal Research Committee. Adult Sprague-Dawley rats (100–300 g, Charles River, Wilmington, MA, RRID:RGD_734476), and wild-type C57BL/6 mice (20–30 g; Jackson Laboratory, Bar Harbor, ME, RRID:IMSR_JAX:000664) of both sexes were used for these studies. Animals were 2-3 months old at the time of the experiments.

Animals were deeply anesthetized with 1–3% isoflurane (Abbott Laboratories, North Chicago, IL), and killed by decapitation or cervical dislocation. The eyes were removed and dissected in Hibernate A (Invitrogen, Carlsbad, CA). For vertical cryosections of the retina, the eyecups were fixed in 4% paraformaldehyde (PFA) in 0.1 M phosphate buffer (PB), pH 7.4, for 15–60 minutes at room temperature (RT). Eyecups were then transferred to 20% sucrose in PB for an hour or 30% sucrose in PB overnight at 4°C. The eyecups were embedded in optimal cutting temperature medium (Sakura Finetek Inc., Torrance, CA) and sectioned at 12–14 μm using a Leica CM3050S or Leica CM 1900 cryostat (Leica Microsystems, Buffalo Grove, IL) and tissue sections were mounted onto gelatin-coated slides. Sections were stored at -20^{o}C until immunostaining.

Whole-mount immunostaining: Retinas were dissected from the eyecup and mounted on cellulose filter paper (EMD Millipore, Temecula, CA) with the GCL up and fixed in 4% PFA for 10 minutes. The whole-mounted retinas were then washed in PB three times for a total of 90 minutes and incubated in 10% normal goat serum at 4°C overnight. The retinas were subsequently incubated in primary antibody (see Table 1) for 5–7 days at 4°C and washed three times for a total of 90 minutes in 0.1 M PB. The retinas were placed in the appropriate secondary antibody overnight at 4°C. After three washes for a total of 90 minutes in PB, the retinas were mounted in Vectashield Mounting Medium (Vector Laboratories, Burlingame, CA). Coverslips were sealed with nail polish. Slides were stored at 4°C and protected from light.

Immunostaining of cryosections of the retina: Retinal sections were incubated in 10% normal donkey serum (NDS) or normal goat serum (NGS) diluted 1:15 in PB with 0.3-0.5% Triton X-100 for 1-2 hours at RT. Sections were then placed in the primary antibody (see Table 1) diluted in PB with 0.3-0.5% Triton X-100 and 0.1% NaN_3 overnight at 4°C. After the primary incubation, the sections were washed three times for a total of 30 minutes in PB and placed in their corresponding secondary antibodies, Alexa Fluor 488-, 555- or 594–rabbit IgG, Alexa Fluor 555–mouse IgG, Alexa Fluor 546–goat IgG, Alexa Fluor 488–rat IgG (Invitrogen) at 1:500-1:1000 dilutions for 2 hours at RT. After a final wash for a total of 30 minutes, the sections were mounted in Vectashield (Vector Laboratories, Burlingame, CA), Aqua Poly/Mount mounting medium (Polysciences, Inc., Warrington, PA) or Citifluor (Citifluor Ltd; London, UK).

To evaluate the specificity of the primary antibody immunostaining, a preadsorption control was performed. Briefly, the $\alpha_2\delta_3$ antibody was diluted in 0.1 M PB containing 0.3% Triton X-100 with a Protein Epitope Signature Tag (PrEST) antigen of human Cacna2d3 (Atlas Antibodies AB, Stockholm, Sweden) at a final concentration of 1 µg/ml for 12 hours at RT. This antigen is fused to a dual tag consisting of the His6 tag and albumin-binding protein. The antibodies directed against the dual tag were depleted before capturing the antigen (Cacna2d3)-specific antibodies in a separate purification step (manufacture's datasheet). No immunostaining was present in sections incubated with the preabsorbed $\alpha_2\delta_3$ subunit antibody, demonstrating the specificity of the antibody (see Results). Except for the $\alpha_2\delta_3$ subunit antibody, all the antibodies employed in this study have been used previously with paraformaldehyde-fixed tissue; our immunostaining patterns were identical to those previously reported earlier (Haverkamp and Wässle, 2000; Deng et al., 2001; Johnson et al., 2003; Martínez-Navarrete et al, 2008; Pérez de Sevilla Müller et al., 2013). Control experiments for non-specific binding of the secondary antibodies omitted the primary antibodies were in both single and double labeling studies.

Antibody characterization (Table 1):

A polyclonal rabbit antibody (cat. #HPA030850; Sigma-Aldrich, St. Louis, MO, RRID:AB_10600764) to the human $\alpha_2\delta_3$ peptide sequence was used to detect $\alpha_2\delta_3$ subunit immunoreactivity. The antibody was characterized by Western blot analysis (Fig. 1B). The antibody detected a single protein band at 123 kDa corresponding to the apparent molecular mass

of the $\alpha_2\delta_3$ subunit under nonreducing conditions (mouse: http://www.uniprot.org/uniprot/Q9Z1L5; rat: http://www.uniprot.org/uniprot/Q8CFG5). Specificity of the $\alpha_2\delta_3$ subunit antibody was also demonstrated in mouse and rat retinal sections incubated in the primary antibody preadsorbed with the $\alpha_2\delta_3$ PrEST antigen. Immunostaining was absent in these sections (see Results).

A mouse monoclonal antibody against the Bassoon protein (cat. #SAP7F407; Enzo Life Sciences, Farmingdale, NY, RRID:AB_10618753) detected a 400 kDa band on a Western blot of the mouse and rat brain (manufacturer's data sheet). The Bassoon monoclonal antibody is a well-established marker of photoreceptor ribbons and immunostaining is not detected in Bassoon knockout retinas (Brandstätter et al.,1999; Dick et al.,2003).

A mouse monoclonal antibody against calbindin (cat. #C9848, cl. CB-955, Sigma-Aldrich, RRID:AB_2314065) was raised against purified bovine kidney calbindin-28K. Calbindin recognized a specific 28 kDa protein on Western blots of mouse brain extracts and immunostaining was absent in the cerebellum of calbindin D-28K knockout mice (manufacturer's data sheet). No cross-reactivity was observed with other EF-hand-containing proteins (e.g., calbindin-9K, calretinin, myosin light chain, parvalbumin, S-100a/b/A2/A6; manufacturer's datasheet). The specificity of this calbindin antibody has been documented previously and it has been used to identify horizontal cells in the rodent retina (Peichl and González-Soriano, 1994; Haverkamp and Wässle, 2000; Hirano et al., 2011).

A goat polyclonal affinity-purified antibody to Chx10 (cat. #sc-21690; Santa Cruz Biotechnology, clone: N-18, Santa Cruz, CA, RRID:AB_2216006) was raised against a peptide corresponding to human $Chx10_{44–61}$ (PPSSHPRAALDGLAPGHL). The Chx10 antibody detects a single 46 kDa band on a Western blot of mouse eye extracts corresponding to the predicted size of Chx10 (manufacturer's datasheet). Chx10 recognizes bipolar cells and a subset of Müller cells in the retina (Liu et al., 1994; Rowan and Cepko, 2004; Elshatory et al., 2007; Whitaker and Cooper, 2009).

A mouse monoclonal antibody against the C-terminal binding protein 2 (CtBP2) (cat. #612044; BD Biosciences, San Jose, CA, RRID:AB_399431) detected a 48 kDa band on a Western blot of rat brain membrane fractions corresponding to the predicted size of CtBP2 (tom Dieck et al., 1998). This monoclonal antibody recognizes synaptic ribbons in photoreceptors and bipolar cells of mouse, cow and monkey retinas (Schmitz et al., 2000; tom Dieck et al., 2005; Jusuf et al., 2006; Puller et al., 2007).

A mouse monoclonal antibody to GAD_{67} (cat. #MAB5406; EMD Millipore,RRID:AB_2278725) detected a single band at 67 kDa on Western blots of rat cortex (Erlander et al., 1991). This antibody does not cross-react with the GAD_{65} isoform in a Western blot of rat cortex (Fong et al., 2005). In addition, immunostaining in the brain showed an overall decrease in a conditional GAD_{67} knockout mutant (Heusner et al., 2008). The antibody stains GABA immunoreactive amacrine cells in the retina (Guo et al., 2010; Delgado et al., 2009).

A rat polyclonal antibody to glycine (cat. #IG1002, ImmunoSolution, Queensland, Australia, RRID:AB_10013222) detected by dot blotting the same amino acid-PFA-thyroglobulin conjugate that was used to immunize the animals. This antibody detected on dot blots conjugates containing glycine, but not conjugates with related amino acids (Pow et al., 1995). Immunostaining was absent following preabsorption with a PFA conjugate of glycine and thyroglobulin (Pow et al., 1995). This antibody selectively immunostains amacrine cells in the retina of multiple species, including mouse and rat (Pow and Hendrickson, 1999; Haverkamp and Wässle, 2000).

A mouse monoclonal antibody to Goα (cat. #MAB3073; EMD Millipore, RRID:AB_94671) detected a single band of 42–43 kDa in homogenates of the olfactory epithelium and the vomeronasal organ in *Xenopus laevis* and *Bufo japonicas* (Hagino-Yamagishi and Nakazawa, 2011). In the retina, Goα is expressed in rod and cone ON-type bipolar cells (Haverkamp and Wässle, 2000; Dhingra et al., 2000).

A guinea pig polyclonal antibody to metabotropic glutamate receptor 6 (mGluR6) (cat. #GP13105; Neuromics, Northfield, MN, RRID:AB_2341540) was raised to a peptide

corresponding to the rat C terminal mGluR6$_{859-871}$ (AAPPQNENAEDAK; manufacture's datasheet). mGluR6 is selectively expressed at the dendritic tips of ON bipolar cells (tom Dieck et al., 2012).

A mouse monoclonal antibody to protein kinase C (PKC) (cat. #K01107M; Biodesign International, Saco, ME, RRID:AB_2313750) was raised against PKCα (79–80 kDa) from purified bovine brain. This antibody reacts with PKC-alpha/beta-1/beta-2 isoforms (manufacturer's data sheet). The PKC antibody recognized the purified PKC protein, as well as an 80 kDa band on Western blots from whole-cell extracts of rat glioma and murine NIH3T3 cell lines. The antibody specifically immunoprecipitates PKC from cell lysates of 328 glioma and SVK 14 cell lines (Young et al.,1988). PKC is a marker for rod bipolar cells in the mouse and rat retina (Haverkamp and Wässle, 2000; Ghosh et al., 2001; Haverkamp et al., 2003). Immunostaining was completely eliminated by the full-length peptide, but was not by unrelated peptides (Young et al., 1988).

A second mouse monoclonal antibody to PKCα (cat. #sc-80, Santa Cruz Biotechnology, RRID:AB_628141) was raised against purified bovine PKC, and its epitope mapped to its hinge region (amino acids 296–317). The antibody recognizes a single band of 80 kDa on Western blots of human cell lines (manufacturer's data sheet) and it has been previously used to demonstrate rod bipolar cells in rodent retinas (Martínez-Navarrete et al., 2007).

A mouse monoclonal antibody to postsynaptic density protein 95 (PSD-95) (cat. #MAB1596, EMD Millipore, RRID:AB_2092365) detected a single band at ~100 kDa, corresponding to the apparent molecular weight of PSD-95 on sodium dodecyl sulfate polyacrylamide gel electrophoresis (SDS-PAGE) immunoblots of rat, mouse, and bovine brain (manufacturer's data sheet). The PSD-95 antibody recognized a major band at ~95 kDa and a minor band at ~80 kDa on Western blots of mouse and rat brain (manufacturer's data sheet). PSD-95 immunoreactivity is localized to photoreceptor terminals and postsynaptically to bipolar cell ribbon synapses in the IPL (Pérez de Sevilla Müller et al., 2013; Koulen at al., 1998).

A guinea pig polyclonal antibody to RNA binding protein with multiple splicing (RBPMS) (cat. #: 1832-RBPMS, PhosphoSolutions, Aurora, CO, RRID:AB_2395389) labeled a single band of the expected molecular size of ~24 kDa on Western blots of mouse and rat retinal extracts. No RBPMS immunostaining was present in tissues incubated with the RBPMS antibodies preabsorbed with $RBPMS_{4-24}$. The affinity purified antibody was shown to exclusively immunostain ganglion cells in mouse and rat retina (Rodriguez et al., 2014).

A mouse monoclonal antibody to the vesicular γ-aminobutyric acid (GABA) transporter (VGAT) (cat. #131 011; Synaptic Systems, Goettingen, Germany, RRID:AB_10890167) recognizes a single band of the expected molecular size of 57 kDa (McIntire et al., 1997; Sagné et al., 1997) on Western blots of mouse brain and retina extracts (Guo et al., 2009). Preadsorption of this antibody with the VGAT N-terminus peptide [$VGAT_{75-87}$ (AEPPVEGDIHYQR)] used for immunization eliminated the VGAT signal on a Western blot (manufacturer's data sheet) and abolished specific VGAT immunolabeling in mouse retina (Guo et al., 2009). This antibody immunostains amacrine and displaced amacrine cells and their processes in the IPL, and horizontal cells and their endings in the OPL in mouse retina (Guo et al., 2009).

A guinea pig polyclonal antibody to the vesicular glutamate transporter 1 (VGluT1) (cat. #AB5905; EMD Millipore, RRID:AB_2301751) recognizes a single band of the expected molecular size of 62 kDa on Western blots of rat hippocampal membranes (McIntire et al., 1997; Sagné et al., 1997; Pacheco Otalora et al., 2006) and immunostains photoreceptor and bipolar cell axon terminals in mouse retina (Bellocchio et al.,1998; Sherry et al., 2003). Preadsorption of the VGluT1 antiserum with the peptide used for the immunization eliminates specific immunostaining (Fyk-Kolodziej et al., 2004). Immunostaining was completely absent in retinae of VGluT1 null mice (Johnson et al., 2007).

RT-PCR: Total RNA was isolated from mouse and rat retina and brain homogenates using the Absolutely RNA Miniprep Kit (Agilent Technologies, Santa Clara CA, USA) according to the manufacturer's instructions. RNA concentrations were determined photometrically. The isolated total RNA (1.0 μg) was used as a template for first-strand cDNA synthesis by using oligo(dT) to prime Superscript III First-Strand Synthesis System for RT-PCR, according to the

manufacturer's instructions (Invitrogen). PCR was performed with primers specific for the $\alpha_2\delta_3$ transcript in rat and mouse, adapted from Schlick et al (2010): forward: 5'-gtatgaatacttcaatgctgtgctg-3' and reverse: 5'-atttaatccctgggtactgtctga-3'. Primer set corresponded to nucleotide positions 381 to 685 in rat and 478 to 782 in mouse, covering exons 4 through 7 of $\alpha_2\delta_3$ mRNA (NCBI Reference Sequences: NM_175595.2 and NM_009785.1, respectively). Expected fragment size was 305 bp.

PCR was performed in a 20 µl reaction volume containing 0.25 µM of each primer, 0.1 units/µl of EconoTaq DNA Polymerase, 400 µM dATP, 400 µM dGTP, 400 µM dCTP and 400 µM dATP, 3 mM $MgCl_2$ (Lucigen Corporation, Middleton, WI, USA) with 2 µl (1/10th) of the cDNA synthesis reaction as template. The following temperature protocol was used: 2 minutes at 96°C, 35 cycles of 30 seconds at 95°C, 30 seconds at 55°C, 1 minute at 72°C, followed by a final extension of 5 minutes at 72°C. 5 µl of the PCR was electrophoresed on a 1.5% agarose gel in 1X TAE (40 mM Tris-acetate, 1 mM EDTA buffer). DNA was visualized using Gel Red (1:10,000) (Biotium, Hayward, CA, USA).

Western Blots: Rodent retina and brain samples were isolated and placed immediately in dH_2O containing 1.5M Tris-HCl, 0.5M EDTA, 0.5M EGTA and 20% Triton X-100 on dry ice. Six mouse retinas or four rat retinas were prepared together. Cell lysis buffer contained 10 µl/ml Halt Protease Inhibitor and 10 µl/ml Halt Phosphatase Inhibitor cocktails (Thermo Fisher Scientific, Waltham, MA, USA). Samples were homogenized for 2 minutes and incubated on ice for 20 minutes to lyse cells. After centrifugation (20,100x*g*; 30 minutes at 4°C), the supernatant fractions were removed. The NanoDrop Spectrophotometer (Thermo Fisher Scientific) was used to measure protein content of the samples. Protein samples were diluted in Laemmli sample buffer, pH 6.8, and samples were boiled for 10 minutes before loading onto the gel.

Western blot analysis of the homogenates was performed after fractionating 35 µg of protein by 4-20% SDS-PAGE (200V for 30 minutes) using Mini-PROTEAN® TGX™ precast polyacrylamide gels (Bio-Rad Laboratories, Hercules, CA, USA). Pre-stained marker proteins were used as molecular mass standards. The separated proteins were transferred to PVDF Immobilon-FL membranes (EMD Millipore) by electroblotting at 360 mA for 2 hours at 4°C.

Blots were allowed to dry completely to increase protein retention before blocking binding sites with a non-mammalian Odyssey Blocker (LI-COR Biosciences, Lincoln, NE) for 45 minutes at RT. Blots were then incubated with $\alpha_2\delta_3$ antibodies (see Table 1) at 1:200 in blocking buffer for 2 hours at RT. Blots were rinsed in a solution containing 0.1 M PB, 0.154 M NaCl and 0.05% Tween 20 (v/v) at pH 7.4 for 30 minutes, and incubated in donkey anti-rabbit IgG conjugated IRDye 680RD (LI-COR) diluted 1:10,000, for 1 hour at RT. The blots were washed and immediately imaged and evaluated using the LI-COR Odyssey® Infrared Imaging System.

Measurements of distances: The linear distance of $\alpha_2\delta_3$ immunoreactive puncta to the closest labeled bipolar and horizontal cell tip, and photoreceptor terminal was measured using Zeiss LSM 510 proprietary software (RRID:SciEx_11637). The line tool was utilized to measure the distance from the outermost portion of immunoreactive $\alpha_2\delta_3$ puncta and the respective closest bipolar or horizontal cell tip. Images were analyzed from single scans taken with a Zeiss Plan-Neofluar 63x 1.4 NA corrected oil objective and a z-axis step of 0.3 or 0.33 μm and a pinhole size of 112 μm. At least ten measurements were taken and averaged.

Fluorescent image acquisition and colocalization analysis: Immunostaining was evaluated using a Zeiss Laser Scanning Microscope 510 Meta, Zeiss LSM 710 (Carl Zeiss, Thornwood, NY, RRID:SciEx_11637) or Leica TCS SP2 laser-scanning confocal microscope (RRID:nlx_156339) with a Zeiss C-Apochromat 40x 1.2 NA corrected water objective, a Zeiss Plan-Neofluar 63x 1.4 NA corrected oil objective or a Leica HCX PL APO 63x/1.4-0.6 Oil Lbd BL at a resolution of 1024×1024 pixels. Images are presented in the figures either as single image scan or as projections of 3–8 image scans (z-axis step between 0.3-0.5 μm). Confocal images were analyzed using Zeiss LSM 510 proprietary software (version 3.2). The intensity levels and contrast of the final images were adjusted in Adobe Photoshop CS2 v.9.02 (Adobe Systems, San Jose, CA).

Results

The $\alpha_2\delta$ subunits are a group of auxiliary calcium channel subunits that modify the properties of the α1 pore-forming and sensor subunit (Davies et al. 2007). In this study, we report the expression and localization of the $\alpha_2\delta_3$ subunit in the mouse and rat retina.

Presence of $\alpha_2\delta_3$ mRNA: From mouse and rat retinal and brain extracts, RT-PCR (n=5 retinas) yielded a strong single band at ~305 bp corresponding to the predicted size of the $\alpha_2\delta_3$ subunit fragment. As a control experiment, water was used in place of template DNA, and no DNA amplification was observed (Fig. 1A). These findings indicate the presence of $\alpha_2\delta_3$ mRNAs in the retina and brain.

Specificity and characterization of the $\alpha_2\delta_3$ subunit antibody

Then, we performed Western blots to determine the presence of the $\alpha_2\delta_3$ subunit protein in the retina. Since $\alpha_2\delta_3$ mRNA is reported in multiple regions of the mouse CNS (Angelotti and Hofmann, 1996; Klugbauer et al., 1999; Gong et al., 2001), the brain was used as a positive control for our Western blots. Western blotting of mouse (n=6 retinas) and rat retina (n=4 retinas) and brain homogenates showed one labeled band corresponded to a molecular weight of ~123 kDa in membrane fractions of mouse and rat brain and retina (Fig. 1B).

Immunohistochemical localization of $\alpha_2\delta_3$ subunit in rodent retinae

$\alpha_2\delta_3$ subunit immunoreactivity was present in cell bodies in the GCL (Fig. 2A, C; arrowheads) and INL (Fig. 2A, C; arrows), and there was weak immunostained processes in the IPL, and strong immunostained puncta in the OPL. The $\alpha_2\delta_3$ subunit immunostaining pattern was similar for both rat (Fig. 2A) and mouse (Fig. 2C) retina. The $\alpha_2\delta_3$ subunit antibody labels cell bodies in the GCL that differ in their size, suggesting multiple retinal ganglion cell (RGC) populations and/or displaced amacrine cells. Immunostained cell bodies located in the proximal INL near the IPL likely correspond to amacrine cells and cell bodies located in the middle of the INL likely correspond to bipolar cells. The strong immunoreactive puncta detected in the OPL of the mouse retina could correspond to photoreceptor terminals. Outer segments of photoreceptors were occasionally stained in both species due to non-specific labeling by the secondary antibody.

Specificity of the antibody was demonstrated by the absence of immunostaining in sections incubated with antibodies preabsorbed with the immunization peptide (Fig. 2B, D).

Identification of $\alpha_2\delta_3$-immunoreactive ganglion and amacrine cells

To characterize the $\alpha_2\delta_3$-expressing cell bodies in the GCL, we immunostained whole-mount retinas from rats (n=7 retinas) and mice (n=5 retinas). The $\alpha_2\delta_3$ subunit immunostaining revealed cell bodies with somal diameters that varied from 7 to 25 µm in the rat (Fig. 3A; n=7 retinas) and mouse (Fig. 3D; n=5 retinas) GCL, suggesting that $\alpha_2\delta_3$-expressing cells belong to different cell populations. Most $\alpha_2\delta_3$-immunoreactive cell bodies in the GCL are likely to be RGCs based on the size of their cell somal diameters. There may also be some displaced amacrine cells that express this subunit based on the presence of some cells with a somal diameter measuring less than 10 µm in diameter (Pérez de Sevilla Müller et al., 2007).

To test if the $\alpha_2\delta_3$-expressing cells in the GCL are RGCs, whole-mounted rat (n=6 retinas) and mouse (n=3 retinas) retinas were immunostained with $\alpha_2\delta_3$ subunit and RBPMS antibodies. RBPMS is a selective marker of all RGCs in rat and mouse retina (Kwong et al., 2010; Rodriguez et al., 2014). All RBPMS-immunoreactive cells contained $\alpha_2\delta_3$ subunit immunoreactivity, indicating that RGCs express this auxiliary Ca subunit in rat (Fig. 3A-C) and mouse (Fig. 3D-F). In addition, many of the small diameter $\alpha_2\delta_3$-immunoreactive cells in the GCL were not RBPMS immunoreactive (Fig. 3C, F, arrows) suggesting they are displaced amacrine cells (Jeon et al., 1998; Pérez de Sevilla Müller et al., 2007; Lin and Masland, 2006; Perry and Walker, 1980; Perry, 1981).

Amacrine cells are composed of multiple types and most express either GABA or glycine immunoreactivity (Wässle and Boycott, 1991; Kay et al., 2011). Vertical sections were stained with antibodies to the glutamic acid decarboxylase 67 isoform (GAD_{67}), a GABA synthesizing enzyme (Schnitzer and Rusoff, 1984). Numerous somata in the GCL and the proximal INL were GAD_{67} immunoreactive in both rat (Fig. 4B) and mouse (Fig. 4E) retina. In the rat retina, ~23% of the GAD_{67} immunostained cells contained $\alpha_2\delta_3$ subunit immunoreactivity in the GCL and in the mouse retina ~42% of the GAD_{67} immunostained cells contained $\alpha_2\delta_3$ subunit immunoreactivity in the GCL (arrowheads). In addition, ~59% and 50% of GAD_{67}

immunostained cell bodies in the GCL did not contain $\alpha_2\delta_3$ subunit immunoreactivity (arrows) in rat and mouse, respectively suggesting the presence of displaced amacrine cells that do not express the $\alpha_2\delta_3$ subunit.

In summary, these findings indicate that $\alpha_2\delta_3$ subunit immunoreactive cells in the GCL are expressed by all RGCs and some displaced amacrine cells.

Characterization of $\alpha_2\delta_3$-immunoreactive cell bodies in the INL

The common amacrine cell markers, GABA and glycine, and the bipolar cell and Müller cell marker, Chx10 were used to determine whether the $\alpha_2\delta_3$-expressing cell bodies in the INL are expressed by amacrine and bipolar cells. In the rat retina, ~60% of the $\alpha_2\delta_3$ subunit immunoreactivity cells contained GAD_{67} in the INL (Fig. 4A-C, arrowheads). In the mouse retina, ~68% of the $\alpha_2\delta_3$ containing cells expressed GAD_{67} immunoreactivity in the INL (Fig. 4D-F, arrowheads). In addition, ~80% and ~53% of GAD_{67} immunostained cell bodies in the INL did not contain $\alpha_2\delta_3$ subunit immunoreactivity (arrows) in rat and mouse, respectively, suggesting the presence of amacrine cells that do not express the $\alpha_2\delta_3$ subunit.

Some $\alpha_2\delta_3$ immunoreactive cell bodies in the proximal INL contain glycine immunoreactivity in rat (Fig. 5A-C, double arrowheads) and mouse (Fig. 6A-C, double arrowheads) retina. The expression of the $\alpha_2\delta_3$ subunit by AII amacrine cells in the rat retina was tested by double immunostaining studies with the parvalbumin (PV) antibody, which labels AII amacrine cells in the rat retina (Wässle et al., 1993). PV-immunoreactive AII amacrine cells do not express the $\alpha_2\delta_3$ subunit (not shown). Immunostaining against glycine also showed bipolar cells in rat, which were not positive for $\alpha_2\delta_3$-expressing bipolar cells (Fig.5A-C (rat) and Fig.6A-C (mouse), arrow), however some $\alpha_2\delta_3$-immunoreactivity could be observed in some glycinergic-bipolar cells [Fig.5A-C (rat) and Fig.6A-C (mouse), arrowhead].

Double label immunostaining studies with antibodies to the $\alpha_2\delta_3$ subunit and Chx10, a pan-bipolar cell and Müller cell marker (Liu et al., 1994; Rowan and Cepko, 2004; Elshatory et al., 2007; Whitaker and Cooper, 2009) were used to evaluate $\alpha_2\delta_3$-immunoreactive bipolar cells. The majority of Chx10-immunoreactive bipolar cells contained $\alpha_2\delta_3$ subunit immunoreactivity in rat

(Fig. 5D-F, arrows) and mouse (Fig. 6D-F, arrows) retina. These findings are consistent with earlier *in situ* hybridization histochemical findings (Nakajima et al. 2009), which report $\alpha_2\delta_3$ subunit mRNAs in mouse bipolar cells. In addition, double immunostaining studies with the antibodies to the $\alpha_2\delta_3$ subunit and PKCα, a marker for rod bipolar cells and DA amacrine cells (Negishi et al., 1998; Haverkamp and Wässle, 2000) revealed $\alpha_2\delta_3$-immunoreactive cell bodies with PKCα immunoreactivity in rat (Fig. 5G-I, arrows) and mouse (Fig. 6G-I, arrows) retina.

In summary, these findings indicate a differential expression of the $\alpha_2\delta_3$ subunit in glycine- and GABA-immunoreactive amacrine cells, and the expression of the $\alpha_2\delta_3$ subunit in most bipolar cells in the rodent retina.

Expression of the $\alpha_2\delta_3$ subunit puncta in the mouse outer retina

To evaluate the localization of the $\alpha_2\delta_3$ subunit in the OPL, we performed double-labeling experiments with specific neuronal markers for bipolar and horizontal cells, and photoreceptors in mouse retina.

The localization of the $\alpha_2\delta_3$ subunit to bipolar cell dendrites was tested by double immunostaining studies with an antibody to PKCα (Fig. 6G-I, arrowheads), to mGluR6, which is localized to the tips of ON-bipolar cell dendrites (tom Dieck et al., 2012; Fig. 7A-D) and to Goα, a marker for ON bipolar cells (Vardi, 1998; Haverkamp and Wässle, 2000; Fig. 7E-H). The $\alpha_2\delta_3$ subunit puncta were adjacent to the bipolar cell tips without any overlap in single sections, suggesting they are not located on the distal dendrites of ON bipolar cells. Most $\alpha_2\delta_3$ subunit puncta were located greater than 0.24±0.09 µm from the nearest ON bipolar cell tip.

To test if $\alpha_2\delta_3$ subunit immunoreactivity is localized to horizontal cells, retinal sections were double immunostained with antibodies to the $\alpha_2\delta_3$ subunit, and to calbindin, a specific horizontal cell marker (Röhrenbeck et al., 1987; Chun and Wässle, 1993; Massey and Mills, 1996; Haverkamp and Wässle, 2000; Hirano et al., 2005) and to VGAT, which is mainly located to horizontal cell endings (Cueva et al., 2002; Guo et al., 2010; Lee and Brecha, 2010). $\alpha_2\delta_3$ immunoreactive puncta were found in the OPL adjacent to horizontal cell processes indicating that they are not expressed by horizontal cells (Fig. 8A-D; Fig. 8E-H). In addition, double

immunostaining with $\alpha_2\delta_3$ and calbindin or VGAT revealed that $\alpha_2\delta_3$ immunoreactive puncta were located at a distance of 0.4±0.1 μm from the closest horizontal cell process.

To test if $\alpha_2\delta_3$ subunit immunoreactivity is localized to photoreceptor terminals, retinal sections were double stained with antibodies to the $\alpha_2\delta_3$ subunit and FITC-peanut agglutinin (PNA), a specific marker for mouse cone pedicle bases (Blanks and Johnson, 1983). Single scan immunohistochemical analysis revealed that the $\alpha_2\delta_3$ subunit is not located at PNA-labeled cone pedicles (Figure 9A-D). The average distance between the closest $\alpha_2\delta_3$ subunit and the PNA-labeled cone pedicle was 1.4±0.2 μm.

Double label studies with antibodies to Bassoon and to CtBP2, which are presynaptic proteins associated with the synaptic ribbon in both rod spherules and cone pedicles (Schmitz et al., 2000; Brandstätter et al., 1999) were used to determine if this subunit is expressed at or near photoreceptor ribbons. Some $\alpha_2\delta_3$ and Bassoon immunoreactive profiles (Fig. 9E-H, arrowheads) overlapped, however, the majority of the $\alpha_2\delta_3$ immunostained puncta were adjacent to Bassoon immunostained puncta, which are located at the base of the synaptic ribbon (Brandstätter et al.,1999) (Fig. 9E-H, arrows). $\alpha_2\delta_3$ immunoreactive puncta were also adjacent or overlapping with CtBP2-immunoreactivity in photoreceptors (Fig. 9I-L, arrows).

Finally, double label studies with antibodies to PSD-95, which is located in the plasma membrane of rod and cone photoreceptor terminals (Koulen et al., 1998; Pérez de Sevilla Müller et al., 2013) and the vesicular glutamate transporter 1 (VGluT1), which is expressed highly in photoreceptor terminals (Johnson et al., 2003; Sherry et al., 2003) were also used to determine if $\alpha_2\delta_3$ subunit immunoreactivity is located at photoreceptor terminals. Single scans of the $\alpha_2\delta_3$ subunit and PSD-95 immunostaining (Fig. 10A-D) and VGluT1 (Fig. 10E-H) showed that PSD-95 and VGluT1 immunoreactive photoreceptor terminals contain all the $\alpha_2\delta_3$ immunoreactive puncta, indicating that the $\alpha_2\delta_3$ puncta in the OPL is located in rod and cone photoreceptor terminals. Together these findings suggest that $\alpha_2\delta_3$ subunits are located at or near the photoreceptor ribbon (see Discussion).

Discussion

The presence of $\alpha_2\delta_1$ (Huang et al., 2013) and $\alpha_2\delta_4$ (Ruether et al., 2000; Wycisk et al., 2006a,b; Mercer et al, 2011; Pérez de Sevilla Müller et al., 2013; Mercer and Thoreson, 2013) Ca channel subunits have been reported in the retina. This study extends these earlier findings and reports the expression of the $\alpha_2\delta_3$ subunit by multiple retinal cell types in the mouse and rat retina. The $\alpha_2\delta_3$ subunit is localized to all RGCs, some displaced amacrine and amacrine cells, rod and cone bipolar cells, and photoreceptors. We did not observe $\alpha_2\delta_3$ subunit immunoreactivity in horizontal cells. Although horizontal cells are the only group of retinal neurons that do not express $\alpha_2\delta_3$ subunits, they do express other calcium channel subunits, including α1C (L-type Ca channel), α1B (N-type Ca channel) and α1A (P/Q-types) subunits (Ueda et al. 1992; Löhrke & Hofmann, 1994; Schubert et al. 2006; Witkovsky et al. 2006; Xue et al., 2013) and the $\alpha_2\delta_1$ subunit (Huang et al., 2013). These subunits are apparently sufficient for mediating calcium channel function in horizontal cells.

$\alpha_2\delta_3$ subunit expression

The $\alpha_2\delta_3$ subunit was initially reported in the brain (Angelotti and Hofmann, 1996; Klugbauer et al., 1999; Gao et al., 2000) and $\alpha_2\delta_3$ subunit mRNA was subsequently reported in mouse retinal bipolar cells by *in situ* hybridization histochemistry (Nakajima et al., 2009). Our findings are consistent with Nakajima's report and extend this observation by showing $\alpha_2\delta_3$ subunit immunoreactivity in RGCs, amacrine cells and photoreceptors.

Possible functional roles of the $\alpha_2\delta_3$ subunit in retinal cells

A well-established role for auxiliary Ca channel subunits is the assembly and trafficking of the α1 pore-forming subunits to the plasma membrane (Arikkath and Campbell, 2003). $\alpha_2\delta$ subunits also participate in synaptogenesis and cytoskeleton formation (Eroglu et al., 2009; Kurshan et al., 2009). Furthermore, the $\alpha_2\delta_3$ subunit participates in presynaptic organization and synaptic transmission at the Drosophila neuromuscular junction (Dickman et al., 2008; Kurshan et al., 2009). In the retina, $\alpha_2\delta_3$ subunits could therefore have multiple roles including (1) regulating the trafficking of the α1 subunit from the soma to the dendritic and axonal endings (Dickman et al., 2008), (2) increasing exocytosis at the presynaptic terminal when Ca^{2+} influx is decreased

(Hoppa et al., 2012) and (3) modifying the biophysical properties of the L-type Ca channels to influence the release of glutamate from photoreceptors and bipolar cells (Heidelberger et al., 2005).

Our study shows that $\alpha_2\delta_3$ subunit is primarily expressed in retinal cell bodies in the rodent retina. Similar immunostaining has been reported for the $\alpha_2\delta_1$ subunit (Huang et al., 2013) which is a neuronal thrombospondin receptor (Eroglu et al., 2009). Thrombospondins have multiple functional roles including synaptic adhesion, cell migration, cytoskeletal dynamics and angiogenesis (Bornstein et al., 2004; Tan and Lawler, 2009). However, it is unknown if the $\alpha_2\delta_3$ subunit also functions as a receptor for thrombospondin proteins.

What α1 subunits are associated with the $\alpha_2\delta_3$ subunit in the retina? Based on the literature there are a few candidates. The L-type Ca channel subunits, α1C and α1D are expressed in photoreceptors and bipolar cells, which are involved in neurotransmission and synaptic plasticity at photoreceptor synapses (Puro et al., 1996; Nachman-Clewner et al., 1999; Xu et al., 2002; Mize at al., 2002) and α1C and α1E subunits are expressed by RGCs and amacrine cells (Sargoy et al., 2014; Xu et al., 2003), which are co-expressed with the auxiliary subunit $\alpha_2\delta_3$ in the mouse brain (Klugbauer et al., 1999). The $\alpha_2\delta_3$ subunit may also interact with the α1F L-type Ca channel subunit localized to rod photoreceptors and bipolar cells. Cacna1F knockout mouse lacks synaptic signaling in the outer retina and shows degeneration of their photoreceptor ribbon terminals (Mansergh et al., 2005; Chang et al., 2006).

$\alpha_2\delta_3$ subunit in retinal diseases

Mice lacking or having mutations of the $\alpha_2\delta$ subunits are characterized by multiple physiological defects, including neurodegeneration, epilepsy, neuropathic pain, cardiovascular dysfunction, and alterations of the biophysical properties of L-type Ca^{2+} currents in cardiomyocytes (Snell, 1955; Fuller-Bicer et al., 2009; Neely et al., 2010). Therefore, it is not surprising that a mutation in the human CACNA2D4 gene, which encodes the $\alpha_2\delta_4$ subunit, results in an outer retinal disease characterized by a reduction of the b-wave, the absence of a photopic ERG, loss of ribbon synapses in rod photoreceptor spherules as well as cone dystrophy (Ruether et al., 2000; Wycisk et al., 2006a, b). A similar distribution of the $\alpha_2\delta_3$ subunit and $\alpha_2\delta_4$ subunit in the OPL of the mouse retina (Pérez de Sevilla Müller et al., 2013; this study), suggests the possibility of

visual system deficits with a mutation or deletion of the $\alpha_2\delta_3$ subunit. However, this suggestion is highly speculative because the structure and electrophysiological properties of Cacna2d3 null mutant retinas have not been evaluated and it is unknown if there are structural or functional alterations in the retina. Further investigation of the Cacna2d3 null mouse line (Neely et al., 2010) is needed for delineating the functional role of the $\alpha_2\delta_3$ subunit in the retina.

Expression of the $\alpha_2\delta_3$ subunit is altered in different diseases. For instance, there is a down regulation of $\alpha_2\delta_2$ subunit expression in most non-small cell lung cancer cell lines (Carboni et al., 2003). Furthermore, previous studies have shown that Cacna2d3 as a reliable marker for malignant childhood neuroblastomas (Thorell et al., 2009; Chu and Best, 2003; Howarth et al., 2012). There is also an up regulation of $\alpha_2\delta_1$ expression in rat spinal dorsal horn and dorsal root ganglia following peripheral nerve injury (Luo et al., 2001; Newton et al., 2001). In generalized progressive retinal atrophy models, where photoreceptor death leads to blindness, current experimental findings indicate that Cacna2d3 mRNA levels are unaltered (Lippmann et al., 2007), which suggests that the $\alpha_2\delta_3$ subunit is a poor marker for retinal disease.

In conclusion, the $\alpha_2\delta_3$ subunit could be involved in transmitter release in ganglion, amacrine, bipolar cells and photoreceptors, as well as trafficking and stabilization of the corresponding α1 calcium channel subunit to their presynaptic sites.

Acknowledgements

We thank Helen Vuong and Dr. Arlene Hirano for their comments and discussion on this project and manuscript.

CONFLICT OF INTEREST STATEMENT

The authors have no conflict of interest.

ROLE OF AUTHORS

All authors had full access to all the data in the study and take responsibility for the integrity of the data and the accuracy of the data analysis. Study concept and design: L.P.S. and N.B. Acquisition of data: L.P.S., A.S., L.F.S., A.R., and J.L. Analysis and interpretation of data: L.P.S., J.L., A.S., A.R., L.F.S., N.C., and N.B. Drafting of the manuscript: L.P.S., A.S., and N.B. Critical revision of the manuscript for important intellectual content: L.P.S. and N.B. Obtained funding: N.B. Administrative, technical, and material support: A.S. and A.R. Study supervision: L.P.S., N.C. and N.B.

References

Angelotti T, Hofmann F.1996. Tissue-specific expression of splice variants of the mouse voltage-gated calcium channel alpha2/delta subunit. FEBS Lett. 397:331-7.

Arikkath J, Campbell KP. 2003. Auxiliary subunits: essential components of the voltage-gated calcium channel complex. Curr Opin Neurobiol.13:298-307.

Barclay J, Balaguero N, Mione M, Ackerman SL, Letts VA, Brodbeck J, Canti C, Meir A, Page KM, Kusumi K, Perez-Reyes E, Lander ES, Frankel WN, Gardiner RM, Dolphin AC, Rees M. 2001. Ducky mouse phenotype of epilepsy and ataxia is associated with mutations in the Cacna2d2 gene and decreased calcium channel current in cerebellar Purkinje cells. J Neurosci. 21:6095-104.

Bauer CS, Tran-Van-Minh A, Kadurin I, Dolphin AC. 2010. A new look at calcium channel α2δ subunits. Curr Opin Neurobiol. 20:563-71.

Bellocchio EE, Hu H, Pohorille A, Chan J, Pickel VM, Edwards RH. 1998. The localization of the brain-specific inorganic phosphate transporter suggests a specific presynaptic role in glutamatergic transmission. J Neurosci 18: 8648–8659.

Blanks JC, Johnson LV. 1983. Selective lectin binding of the developing mouse retina. J Comp Neurol 221:31-41.

Brandstätter JH, Fletcher EL, Garner CC, Gundelfinger ED, Wässle H. 1999. Differential expression of the cytomatrix protein bassoon among ribbon synapses in the mammalian retina. Eur J Neurosci 11:3683–3693.

Brodbeck J, Davies A, Courtney JM, Meir A, Balaguero N, Canti C, Moss FJ, Page KM, Pratt WS, Hunt SP, Barclay J, Rees M, Dolphin AC. 2002. The ducky mutation in Cacna2d2 results in altered Purkinje cell morphology and is associated with the expression of a truncated alpha 2 delta-2 protein with abnormal function. J Biol Chem 277:7684-93.

Carboni GL, Gao B, Nishizaki M, Xu K, Minna JD, Roth JA, Ji L. 2003. CACNA2D2-mediated apoptosis in NSCLC cells is associated with alterations of the intracellular calcium signaling and disruption of mitochondria membrane integrity. Oncogene 22:615-26.

Caterall 2000. Structure and regulation of voltage-gated Ca2+ channels. Annu Rev Cell Dev Biol 16:521-555.

Chu PJ, Best PM. 2003. Molecular cloning of calcium channel alpha(2)delta-subunits from rat atria and the differential regulation of their expression by IGF-1. J Mol Cell Cardiol. 35:207-15.

Chun MH, Wässle H. 1993. Some horizontal cells of the bovine retina receive input synapses in the inner plexiform layer. Cell Tissue Res. 272:447-57.

Cole RL, Lechner SM, Williams ME, Prodanovich P, Bleicher L, Varney MA, Gu G. 2005. Differential distribution of voltage-gated calcium channel α2-δ (α2δ) subunit mRNA-containing cell in the rat central nervous system and the dorsal root ganglia. J Comp Neurol 491:246-269.

Cueva JG, Haverkamp S, Reimer RJ, Edwards R, Wässle H, Brecha NC. 2002. Vesicular gamma-aminobutyric acid transporter expression in amacrine and horizontal cells. J Comp Neurol 445:227-37.

Davies A, Hendrich J, Van Minh AT, Wratten J, Douglas L, Dolphin AC. 2007. Functional biology of the alpha(2)delta subunits of voltage-gated calcium channels. Trends Pharmacol Sci. 28:220-8.

Delgado LM1, Vielma AH, Kähne T, Palacios AG, Schmachtenberg O. 2009. The GABAergic system in the retina of neonate and adult Octodon degus, studied by immunohistochemistry and electroretinography. J Comp Neurol. 2009 514:459-72.

Deng P, Cuenca N, Doerr T, Pow DV, Miller R, Kolb H. 2001. Localization of neurotransmitters and calcium binding proteins to neurons of salamander and mudpuppy retinas. Vision Res. 41:1771-83.

Dhingra A, Lyubarsky A, Jiang M, Pugh EN Jr, Birnbaumer L, Sterling P, Vardi N. 2000. The light response of ON bipolar neurons requires Gαo. J Neurosci. 20:9053-8.

Dick O, tom Dieck S, Altrock WD, Ammermüller J, Weiler R, Garner CC, Gundelfinger ED, Brandstätter JH. 2003. The presynaptic active zone protein bassoon is essential for photoreceptor ribbon synapse formation in the retina. Neuron 37:775-86.

Dickman DK, Kurshan PT, Schwarz TL. 2008. Mutations in a Drosophila alpha2delta voltage-gated calcium channel subunit reveal a crucial synaptic function. J Neurosci. 28:31-38.

Dolphin AC. 2012. Calcium channel auxiliary α2δ and β subunits: trafficking and one step beyond. Nat Rev Neurosci. 13:542-55.

Elshatory Y1, Everhart D, Deng M, Xie X, Barlow RB, Gan L. 2007. Islet-1 controls the differentiation of retinal bipolar and cholinergic amacrine cells. J Neurosci. 27:12707-20.

Erlander MG, Tillakaratne NJ, Feldblum S, Patel N, Tobin AJ. 1991. Two genes encode distinct glutamate decarboxylases. Neuron 7:91–100.

Eroglu C, Allen NJ, Susman MW, O'Rourke NA, Park CY, Ozkan E, Chakraborty C, Mulinyawe SB, Annis DS, Huberman AD, Green EM, Lawler J, Dolmetsch R, Garcia KC, Smith SJ, Luo ZD, Rosenthal A, Mosher DF, Barres BA. 2009. Gabapentin receptor alpha2delta-1 is a neuronal thrombospondin receptor responsible for excitatory CNS synaptogenesis. Cell 139:380-392.

Fyk-Kolodziej B, Dzhagaryan A, Qin P, Pourcho RG. 2004. Immunocytochemical localization of three vesicular glutamate transporters in the cat retina. J Comp Neurol 475: 518–530.

Fong AY1, Stornetta RL, Foley CM, Potts JT. 2005. Immunohistochemical localization of GAD67-expressing neurons and processes in the rat brainstem: subregional distribution in the nucleus tractus solitarius. J Comp Neurol. 493:274-90.

Fuller-Bicer GA, Varadi G, Koch SE, Ishii M, Bodi I, Kadeer N, Muth JN, Mikala G, Petrashevskaya NN, Jordan MA, Zhang SP, Qin N, Flores CM, Isaacsohn I, Varadi M, Mori Y, Jones WK, Schwartz A. 2009. Targeted disruption of the voltage-dependent calcium channel alpha2/delta-1-subunit. Am J Physiol Heart Circ Physiol. 297:H117-24.

Gao B, Sekido Y, Maximov A, Saad M, Forgacs E, Latif F, Wei MH, Lerman M, Lee JH, Perez-Reyes E, Bezprozvanny I, Minna JD. 2000. Functional properties of a new voltage-dependent calcium channel a2d auxiliary subunit gene (CACNA2D2). J Biol Chem 275:12237-42.

Gong HC, Hang J, Kohler W, Li L, Su TZ. 2001. Tissue-specific expression and gabapentin-binding proteins properties of calcium channel subunit alpha2delta subunit subtypes. J membr biol 184:35-43.

Ghosh KK, Haverkamp S, Wassle H. 2001. Glutamate receptors in the rod pathway of the mammalian retina. J Neurosci. 21:8636-47.

Guo C, Stella SL, Hirano AA, and Brecha N. 2009. Plasmalemmal and vesicular-aminobutyric acid transporter expression in the developing mouse retina. J Comp Neurol 512:6–26.

Guo C, Hirano AA, Stella SL, Bitzer M, Brecha NC. 2010. Guinea pig horizontal cells express GABA, the GABA-synthesizing enzyme GAD65, and the GABA vesicular transporter. J Comp Neurol 518:1647-69.

Hagino-Yamagishi K, Nakazawa H. 2011. Involvement of Gα(olf)-expressing neurons in the vomeronasal system of Bufo japonicus. J Comp Neurol 519:3189-201.

Haverkamp S, Wässle H. 2000. Immunocytochemical analysis of the mouse retina. J Comp Neurol 424:1–23.

Haverkamp S, Ghosh KK, Hirano AA, Wässle H. 2003. Immunocytochemical description of five bipolar cell types of the mouse retina. J Comp Neurol. 455:463– 476.

Heidelberger, R., Thoreson, W.B., and Witkovsky, P. 2005. Synaptic transmission at retinal ribbon synapses. Prog Retin Eye Res. 24:682–720.

Heusner CL1, Beutler LR, Houser CR, Palmiter RD. 2008. Deletion of GAD67 in dopamine receptor-1 expressing cells causes specific motor deficits. Genesis. 46:357-67.

Hirano AA, Brandstätter JH, Brecha NC. 2005. Cellular distribution and subcellular localization of molecular components of vesicular transmitter release in horizontal cells of rabbit retina. J Comp Neurol. 488:70-81.

Hirano AA, Brandstätter JH, Morgans CW, Brecha NC. 2011. SNAP25 expression in mammalian retinal horizontal cells. J Comp Neurol. 519:972-88.

Hoppa MB, Lana B, Margas W, Dolphin AC, Ryan TA. 2012. $\alpha_2\delta$ expression sets presynaptic calcium channel abundance and release probability. Nature. 486:122-5.

Howarth FC, Qureshi MA, Hassan Z, Isaev D, Parekh K, John A, Oz M, Raza H, Adeghate E, Adrian TE. 2012. Contractility of ventricular myocytes is well preserved despite altered mechanisms of Ca2+ transport and a changing pattern of mRNA in aged type 2 Zucker diabetic fatty rat heart. Mol Cell Biochem. 361:267-80.

Huang J, Zhou L, Wang H, Luo J, Zeng L, Xiong K, Chen D. 2013. Distribution of thrombospondins and their neuronal receptor α2δ1 in the rat retina. Exp Eye Res. 111:36-49.

Jeon CJ, Strettoi E, Masland RH. 1998. The major cell populations of the mouse retina. J Neurosci. 18:8936-46.

Johnson J, Tian N, Caywood MS, Reimer RJ, Edwards RH, Copenhagen DR. 2003. Vesicular neurotransmitter transporter expression in developing postnatal rodent retina: GABA and glycine precede glutamate. J Neurosci. 23:518e529.

Johnson J, Fremeau RT, Jr., Duncan JL, Renteria RC, Yang H, Hua Z, Liu X, LaVail MM, Edwards RH, Copenhagen DR. 2007.Vesicular glutamate transporter 1 is required for photoreceptor synaptic signaling but not for intrinsic visual functions. J Neurosci. 27:7245–7255.

Jusuf PR, Martin PR, Grünert U. 2006. Synaptic connectivity in the midget-parvocellular pathway of primate central retina. J Comp Neurol. 494:260–274.

Kay JN, Voinescu PE, Chu MW, Sanes JR. 2011. Neurod6 expression defines new retinal amacrine cell subtypes and regulates their fate. Nat Neurosci. 14:965-72.

Klugbauer N, Lacinová L, Marais E, Hobom M, Hofmann F. 1999. Molecular diversity of the calcium channel α2δ subunit. J Neurosci. 19:684-691.

Koulen P, Fletcher EL, Craven SE, Bredt DS, Wässle H. 1998. Immunocytochemical localization of the postsynaptic density protein PSD-95 in the mammalian retina. J Neurosci. 18:10136-49.

Kurshan PT, Oztan A, Schwarz TL. 2009. Presynaptic alpha(2)delta-3 is required for synaptic morphogenesis independent of its Ca(2+)-channel functions. Nat Neurosci. 12:1415-23.

Kwong JM1, Caprioli J, Piri N. 2010. RNA binding protein with multiple splicing: a new marker for retinal ganglion cells. Invest Ophthalmol Vis Sci. 51:1052-8.

Lee H, Brecha NC. 2010. Immunocytochemical evidence for SNARE protein-dependent transmitter release from guinea pig horizontal cells. Eur J Neurosci. 31:1388-401.

Lin B, Masland RH. 2006. Populations of wide-field amacrine cells in the mouse retina. J Comp Neurol. 499:797-809.

Lippmann T, Jonkisz A, Dobosz T, Petrasch-Parwez E, Epplen JT, Dekomien G. 2007. Haplotype-defined linkage region for gPRA in Schapendoes dogs. Mol Vis. 13:174-80.

Liu X, Hirano AA, Sun X, Brecha NC, Barnes S. 2013. Calcium channels in rat horizontal cells regulate feedback inhibition of photoreceptors through an unconventional GABA- and pH-sensitive mechanism. J Physiol. 591:3309-24.

Liu IS, Chen JD, Ploder L, Vidgen D, van der Kooy D, Kalnins VI, McInnes RR. 1994. Developmental expression of a novel murine homeobox gene (Chx10): evidence for roles in determination of the neuroretina and inner nuclear layer. Neuron 13:377-93.

Löhrke S, Hofmann HD. 1994. Voltage-gated currents of rabbit A- and B-type horizontal cells in retinal monolayer cultures. Vis Neurosci 2, 369–378.

Luo ZD, Chaplan SR, Higuera ES, Sorkin LS, Stauderman KA, Williams ME, Yaksh TL. 2001. Upregulation of dorsal root ganglion (alpha)2(delta) calcium channel subunit and its correlation with allodynia in spinal nerve-injured rats. J Neurosci. 21:1868-75.

Martínez-Navarrete GC, Martín-Nieto J, Esteve-Rudd J, Angulo A, Cuenca N. 2007. α-Synuclein gene expression profile in the retina of vertebrates. Mol Vis. 13: 949–961.

Martínez-Navarrete GC, Angulo A, Martín-Nieto J, Cuenca N. 2008. Gradual morphogenesis of retinal neurons in the peripheral retinal margin of adult monkeys and humans. J Comp Neurol. 511:557-80.

Massey SC, Mills SL. 1996. A calbindin-immunoreactive cone bipolar cell type in the rabbit retina. J Comp Neurol. 366:15-33.

McIntire SL, Reimer RJ, Schuske K, Edwards RH, Jorgensen EM. 1997. Identification and characterization of the vesicular GABA transporter. Nature 389:870-876.

Mercer AJ, Chen M, Thoreson WB. 2011. Lateral mobility of presynaptic L-type calcium channels at photoreceptor ribbon synapses. J Neurosci. 31:4397-406.

Mercer AJ, Thoreson WB. 2013. Tracking quantum dot-tagged calcium channels at vertebrate photoreceptor synapses: retinal slices and dissociated cells. Curr Protoc Neurosci. Chapter 2:Unit 2.18.

Mize RR, Graham SK, Cork RJ. 2002. Expression of the L-type calcium channel in the developing mouse visual system by use of immunocytochemistry. Brain Res Dev Brain Res. 136:185–195.

Nachman-Clewner M, St Jules R, Townes-Anderson E. 1999. L-type calcium channels in the photoreceptor ribbon synapse: localization and role in plasticity. J Comp Neurol. 415:1–16.

Nakajima Y, Moriyama M, Hattori M, Minato N, Nakanishi S. 2009. Isolation of ON bipolar cell genes via hrGFP-coupled cell enrichment using the mGluR6 promoter. J Biochem. 145:811-8.

Neely GG, Hess A, Costigan M, Keene AC, Goulas S, Langeslag M, Griffin RS, Belfer I, Dai F, Smith SB, Diatchenko L, Gupta V, Xia CP, Amann S, Kreitz S, Heindl-Erdmann C, Wolz S, Ly CV, Arora S, Sarangi R, Dan D, Novatchkova M, Rosenzweig M, Gibson DG, Truong D, Schramek D, Zoranovic T, Cronin SJ, Angjeli B, Brune K, Dietzl G, Maixner W, Meixner A, Thomas W, Pospisilik JA, Alenius M, Kress M, Subramaniam S, Garrity PA, Bellen HJ, Woolf CJ, Penninger JM. 2010. A genome-wide Drosophila screen for heat nociception identifies $\alpha_2\delta_3$ as an evolutionarily conserved pain gene. Cell. 143:628-38.

Negishi K, Kato S, Teranishi T. 1988. Dopamine cells and rod bipolar cells contain protein kinase C-like immunoreactivity in some vertebrate retinas. Neurosci Lett. 94:247-52.

Newton RA, Bingham S, Case PC, Sanger GJ, Lawson SN. 2001. Dorsal root ganglion neurons show increased expression of the calcium channel alpha2delta-1 subunit following partial sciatic nerve injury. Brain Res Mol Brain Res. 95:1-8.

Pacheco Otalora LF, Couoh J, Shigamoto R, Zarei MM, Garrido Sanabria ER. 2006. Abnormal mGluR2/3 expression in the perforant path termination zones and mossy fibers of chronically epileptic rats. Brain Res 1098: 170–185.

Peichl L, González-Soriano J. 1994. Morphological types of horizontal cell in rodent retinae: a comparison of rat, mouse, gerbil, and guinea pig. Vis Neurosci. 11:501-17.

Pérez de Sevilla Müller L, Shelley J, Weiler R. 2007. Displaced amacrine cells of the mouse retina. J Comp Neurol. 505:177-89.

Pérez de Sevilla Müller L, Liu J, Solomon A, Rodriguez A, Brecha NC. 2013. Expression of voltage-gated calcium channel α(2)δ(4) subunits in the mouse and rat retina. J Comp Neurol. 521:2486-501.

Perry VH, Walker M. 1980. Amacrine cells, displaced amacrine cells and interplexiform cells in the retina of the rat. Proc R Soc Lond B Biol Sci. 208:415-31.

Perry VH. 1981. Evidence for an amacrine cell system in the ganglion cell layer of the rat retina. Neuroscience. 6:931-44.

Pow DV, Wright LL, Vaney DI. 1995. The immunocytochemical detection of amino-acid neurotransmitters in paraformaldehyde-fixed tissues. J Neurosci Methods. 56:115-123.

Pow DV1, Hendrickson AE. 1999. Distribution of the glycine transporter glyt-1 in mammalian and nonmammalian retinae. Vis Neurosci. 16:231-9.

Puller C, Haverkamp S, Grünert U. 2007. OFF midget bipolar cells in the retina of the marmoset, Callithrix jacchus, express AMPA receptors. J Comp Neurol. 502:442–454.

Puro DG, Hwang JJ, Kwon OJ, Chin H. 1996. Characterization of an L-type calcium channel expressed by human retinal Muller (glial) cells. Brain Res Mol Brain Res. 37:41–48.

Röhrenbeck J, Wässle H, Heizmann CW. 1987. Immunocytochemical labelling of horizontal cells in mammalian retina using antibodies against calcium-binding proteins. Neurosci Lett. 77:255-60.

Rodriguez AR, Pérez de Sevilla Müller L, Brecha NC. 2014. The RNA binding protein RBPMS is a selective marker of ganglion cells in the mammalian retina. J Comp Neurol. 522:1411-43.

Rowan S, Cepko CL. 2004. Genetic analysis of the homeodomain transcription factor Chx10 in the retina using a novel multifunctional BAC transgenic mouse reporter. Dev Biol. 271:388-402.

Ruether K, Grosse J, Matthiessen E, Hoffman K, Hartmann C. 2000. Abnormalities of the photoreceptor-bipolar cell synapse in a substrain of C57BL/10 mice. Invest Opththalmol Vis Sci. 41:4039-4047.

Sargoy A, Sun X, Barnes S, Brecha NC. 2014. Differential calcium signaling mediated by voltage-gated calcium channels in rat retinal ganglion cells and their unmyelinated axons. PLoS One. 9:e84507.

Sagné C, El Mestikawy S, Isambert MF, Hamon M, Henry JP, Giros B, Gasnier B. 1997. Cloning of a functional vesicular GABA and glycine transporter by screening of genome databases. FEBS Lett. 417:177–183.

Schlick B, Flucher BE, and Obermair GJ. 2010. Voltage-activated calcium channel expression profiles in mouse brain and cultured hippocampal neurons. Neuroscience 167:786-98.

Schmitz F, Königstorfer A, Südhof TC. 2000. RIBEYE, a component of synaptic ribbons: a protein's journey through evolution provides insight into synaptic ribbon function. Neuron 28:857–872.

Schnitzer J, Rusoff AC. 1984. Horizontal cells of the mouse retina contain glutamic acid decarboxylase-like immunoreactivity during early developmental stages. J Neurosci. 4:2948-2955.

Schubert T, Weiler R, Feigenspan A. 2006. Intracellular calcium is regulated by different pathways in horizontal cells of the mouse retina. J Neurophysiol 96:1278–1292.

Sherry DM, Wang MM, Bates J, Frishman LJ. 2003. Expression of vesicular glutamate transporter 1 in the mouse retina reveals temporal ordering in development of rod vs. cone and ON vs. OFF circuits. J Comp Neurol. 465: 480–498.

Snell GD. 1955. Ducky, a new second chromosome mutation in the mouse. J Hered. 46:27-29.

Taylor CP1, Garrido R. 2008. Immunostaining of rat brain, spinal cord, sensory neurons and skeletal muscle for calcium channel alpha2-delta (alpha2-delta) type 1 protein. Neuroscience. 155:510-21.

Thorell K1, Bergman A, Carén H, Nilsson S, Kogner P, Martinsson T, Abel F. 2009. Verification of genes differentially expressed in neuroblastoma tumours: a study of potential tumour suppressor genes. BMC Med Genomics. 2:53.

tom Dieck S, Sanmarti-Vila L, Langnaese K, Richter K, Kindler S, Soyke A, Wex H, Smalla KH, Kampf U, Franzer JT, Stumm M, Garner CC, Gundelfinger ED. 1998. Bassoon, a novel zinc-finger AG/glutaminerepeat protein selectively localized at the active zone of presynaptic nerve terminals. J Cell Biol. 142:499–509.

tom Dieck S, Altrock WD, Kessels MM, Qualmann B, Regus H, Brauner D, Fejtova A, Bracko O, Gundelfinger ED, Brandstätter JH. 2005. Molecular dissection of the photoreceptor ribbon

synapse: physical interaction of bassoon and RIBEYE is essential for the assembly of the ribbon complex. J Cell Biol. 168:825–836.

tom Dieck S, Specht D, Strenzke N, Hida Y, Krishnamoorthy V, Schmidt KF, Inoue E, Ishizaki H, Tanaka-Okamoto M, Miyoshi J, Hagiwara A, Brandstätter JH, Löwel S, Gollisch T, Ohtsuka T, Moser T. 2012. Deletion of the presynaptic scaffold CAST reduces active zone size in rod photoreceptors and impairs visual processing. J Neurosci. 32:12192-203.

Ueda Y, Kaneko A, Kaneda M. 1992. Voltage-dependent ionic currents in solitary horizontal cells isolated from cat retina. J Neurophysiol 4:1143–1150.

Vardi N. 1998. Alpha subunit of Go localizes in the dendritic tips of ON bipolar cells. J Comp Neurol. 395:43–52.

Wanajo A, Sasaki A, Nagasaki H, Shimada S, Otsubo T, Owaki S, Shimizu Y, Eishi Y, Kojima K, Nakajima Y, Kawano T, Yuasa Y, Akiyama Y. 2008. Methylation of the calcium channel-related gene, CACNA2D3, is frequent and a poor prognostic factor in gastric cancer. Gastroenterology. 135:580-590.

Wässle H, Grünert U, Röhrenbeck J. 1993. Immunocytochemical staining of AII-amacrine cells in the rat retina with antibodies against parvalbumin. J Comp Neurol. 332:407-20.

Wässle H. 2004. Parallel processing in the mammalian retina. Nat Rev Neurosci. 5:747-57.

Wässle H, Boycott BB. 1991. Functional architecture of the mammalian retina. Physiol Rev. 71:447-80.

Whitaker CM1, Cooper NG. 2009. The novel distribution of phosphodiesterase-4 subtypes within the rat retina. Neuroscience 163:1277-91.

Witkovsky P, Shen C, McRory J. 2006. Differential distribution of voltage-gated calcium channels in dopaminergic neurons of the rat retina. J Comp Neurol 497:384–396.

Wycisk KA, Budde B, Feil S, Skosyrski S, Buzzi F, Neidhardt J, Glaus E, Nürnberg P, Ruether K, Berger W. 2006a. Structural and functional abnormalities of retinal ribbon synapses due to Cacna2d4 mutation. Invest Ophthalmol Vis Sci. 47:3523-30.

Wycisk KA, Zeitz C, Feil S, Wittmer M, Forster U, Neidhardt J, Wissinger B, Zrenner E, Wilke R, Kohl S, Berger W. 2006b. Mutation in the auxiliary calcium-channel subunit Cacna2d4 causes autosomal recessive cone dystrophy. Am J Hum Genet. 79:973-7.

Xu HP, Zhao JW, Yang XL. 2002. Expression of voltage-dependent calcium channel subunits in the rat retina. Neurosci Lett. 329:297-300.

Xu HP, Zhao JW, Yang XL. 2003. Cholinergic and dopaminergic amacrine cells differentially express calcium channel subunits in the rat retina. Neuroscience 118:763-8.

Young S, Rothbard J, Parker PJ. 1988. A monoclonal antibody recognizing the site of limited proteolysis of protein kinase C. Eur J Biochem. 173:247–252.

Figure legends

Figure 1. Expression of the voltage-gated accessory calcium channel $\alpha_2\delta_3$ subunit mRNA and protein in mouse and rat brain and retina extracts. (A) RT-PCR $\alpha_2\delta_3$ subunit. (B) Western blots using the $\alpha_2\delta_3$ antibody in the mouse and rat retina and brain homogenates. A protein band of ~123 kDa was detected in these tissues. Ms=Mouse, R=Retina, B=Brain.

Figure 2. Localization of $\alpha_2\delta_3$ accesory calcium channel subunit immunoreactivity in the rodent retina. (A) Expression of $\alpha_2\delta_3$ subunit in the rat retina. $\alpha_2\delta_3$ immunostaining was in cells in the GCL (arrowheads), INL (arrows) and processes in the OPL. (B) No staining was observed in retinas incubated with antibodies preadsorbed with the immunization peptide. (C) Expression of $\alpha_2\delta_3$ subunit in the mouse retina. $\alpha_2\delta_3$ immunostaining was in cells in the GCL (arrowheads) and INL (arrows) and with strong immunoreactive puncta in the OPL. (D) No staining was observed in mouse section incubated with the blocking peptide as a control for the specificity of the antibody. ONL: outer nuclear layer; OPL: outer plexiform layer; INL: inner nuclear layer; IPL: inner plexiform layer; GCL: ganglion cell layer. Scale bars: 20 μm.

Figure 3: $\alpha_2\delta_3$ immunoreactivity (green) was expressed in RBPMS (magenta)-containing cells in the rat (A-C) and mouse (D-F) GCL. RBPMS is a selective marker for RGCs. Arrows indicate cells containing $\alpha_2\delta_3$ immunoreactivity and no RBPMS immunoreactivity, indicating that they are displaced amacrine cells. Scale bars: 50 μm.

Figure 4: Localization of GAD_{67} and $\alpha_2\delta_3$ subunit immunoreactivities in the rodent retina. (A) $\alpha_2\delta_3$ immunostaining (green) in the rat retina. (B) GAD_{67} (magenta) immunolabeled IPL, OPL, and cell bodies in the proximal INL and GCL. (C) Merge image showing that some (arrowheads) but not all GAD_{67} (arrows) express the $\alpha_2\delta_3$ subunit in the GCL and INL. (D) $\alpha_2\delta_3$ immunostaining (green) in the mouse retina. (E) GAD_{67} (magenta) and (F) merge image showing colocalization of the $\alpha_2\delta_3$ subunit (arrowheads) with some but not all GAD_{67} amacrine cells (arrows) in the GCL and INL. OPL: outer plexiform layer; INL: inner nuclear layer; IPL: inner plexiform layer; GCL: ganglion cell layer. Scale bar (A-H): 20 μm.

Figure 5: Localization of $\alpha_2\delta_3$ subunit in bipolar cells of the rat retina. (A) $\alpha_2\delta_3$ immunostaining (green) in the rat retina. (B) Immunostaining against glycine (magenta) stained bipolar cells

through gap junctions with AII cells and revealed that some ON bipolar cells were immunostained by $\alpha_2\delta_3$ subunit antibodies (A-C, arrowheads) while other ON bipolar cells were not (arrows). Some glycinergic amacrine cells were positive for $\alpha_2\delta_3$ immunostaining (double arrowheads). (D) $\alpha_2\delta_3$ immunostaining (green) in the rat retina. (E) Chx10 (magenta), a pan-bipolar cell marker. (F) Colocalization of $\alpha_2\delta_3$ in some bipolar cells in the cell body (arrows). (G) $\alpha_2\delta_3$ immunostaining (green) in the rat retina. The immunostaining with PKCα antibody (magenta), a marker for rod bipolar cells (H), revealed co-localization with $\alpha_2\delta_3$ in rod bipolar cells (G-I, arrows). OPL: outer plexiform layer; INL: inner nuclear layer; IPL: inner plexiform layer. Scale bar: 10 μm.

Figure 6: Localization of $\alpha_2\delta_3$ subunit in bipolar cells of the mouse retina. (A) $\alpha_2\delta_3$ immunostaining (green) in the mouse retina. (B) Glycine antibody immunostaining (magenta) revealed that some ON bipolar cells were immunostained by $\alpha_2\delta_3$ subunit antibodies (A-C, arrowheads) while other ON bipolar cells were not (arrows). Some glycinergic amacrine cells were positive for $\alpha_2\delta_3$ immunostaining (double arrowheads). (D) $\alpha_2\delta_3$ immunostaining (green) in the mouse retina. (E) Chx10 (magenta), a pan-bipolar cell marker. (F) Colocalization of $\alpha_2\delta_3$ in some bipolar cell bodies (arrows). (G) $\alpha_2\delta_3$ immunostaining (green) in the mouse retina. The immunostaining with PKCα antibody (magenta), a marker for rod bipolar cells (H), revealed co-localization with $\alpha_2\delta_3$ in rod bipolar cells (G-I, arrows) but was absent in the distal dendrites (arrowheads). OPL: outer plexiform layer; INL: inner nuclear layer; IPL: inner plexiform layer. Scale bar: 10 μm.

Figure 7. $\alpha_2\delta_3$ accessory calcium channel subunit is not in bipolar cell tips in the OPL of the mouse retina. (A) Double immunostaining of retinal sections with mGluR6 (green) and $\alpha_2\delta_3$ (magenta). (B-D) High magnification of single scan showing that mGluR6 immunoreactivity does not co-localize with the $\alpha_2\delta_3$ accessory calcium channel subunit (arrows). (E) Go_α-immunoreactivity (green) and $\alpha_2\delta_3$-immunoreactivity subunit (magenta). (F-H) High-power image (boxed area from E) showing that Goα-immunoreactivity and $\alpha_2\delta_3$ subunit do not colocalized (arrows). Z-step = 0.33 μm. Scale bars (A, B): 20 μm, (B-D, F-H): 5 μm.

Figure 8. $\alpha_2\delta_3$ accessory calcium channel subunit is not expressed by horizontal cells in the mouse retina. (A) Single scan (boxed area from A) showing horizontal cells with calbindin and

$\alpha_2\delta_3$ subunit staining (magenta). (B-D) High magnification of single scan showing $\alpha_2\delta_3$ subunit and horizontal cell processes. $\alpha_2\delta_3$ subunit was never found to be colocalized with horizontal cells or their processes. (E) Single scan showing horizontal cells tips labeled with a VGAT antibody (green) and $\alpha_2\delta_3$ subunit staining (magenta). (F-H) High magnification (boxed area from E) of single scan showing $\alpha_2\delta_3$ subunit staining. Z-step = 0.33 μm. Scale bar in (A, E): 20 μm, (B-D, F-H): 5 μm.

Figure 9. $\alpha_2\delta_3$ accessory calcium channel subunit in photoreceptors of the mouse retina. (A) Labeling of cone pedicles with PNA–FITC and $\alpha_2\delta_3$ accessory calcium channel subunit. (B-D) High magnification of single scan indicating that $\alpha_2\delta_3$ subunit is not located in the base of cone pedicles. (E) Double immunolabeling of $\alpha_2\delta_3$ accessory calcium channel subunits (magenta) and Bassoon (green), a presynaptic protein. (F-H) High magnification (boxed area from E) showing colocalization of some $\alpha_2\delta_3$ subunits (arrowheads). (I) Double immunolabeling of $\alpha_2\delta_3$ accessory calcium channel subunits (magenta) and CtBP2 (green), a ribbon synapse marker. (J-L) High magnification (boxed area from I) showing that a few of the $\alpha_2\delta_3$ subunits are adjacent to CtBP2 (arrows). Z-step = 0.33 μm. Scale bars (A, E, I): 20 μm; (B-D, F-H, J-L): 5 μm.

Figure 10. $\alpha_2\delta_3$ accessory calcium channel subunit in photoreceptors of the mouse retina. (A) Double immunolabeling of postsynaptic density protein 95 (PSD-95) (green) and $\alpha_2\delta_3$ subunit (magenta) in the mouse retina. (B-D): High-magnification view (boxed area from A) showing that all $\alpha_2\delta_3$ immunoreactive puncta were distributed inside the photoreceptor terminals. (E) Double immunolabeling of VGluT1 (green) for photoreceptor axon terminals and $\alpha_2\delta_3$ subunit (magenta) in the mouse retina. (F-H): High-magnification view (boxed area from E) showing that $\alpha_2\delta_3$ immunoreactive puncta are located inside the photoreceptor terminals. Z-step = 0.33 μm. Scale bars (A, E): 20 μm; (B-D, F-H): 5 μm.

Antibody	Antigen/immunogen	Species/dilution	Source/catalog No./ RRID No.
$\alpha_2\delta_3$	Calcium channel, voltage-dependent, α-2/δ subunit 3 recombinant protein epitope signature tag (PrEST). Immunogen sequence SCDDETVNCYLIDNNGFILVSEDYTQ TGDFFGEIEGAVMNKLLTMGSFKRITLYDYQAMCRA NKESSDG	Rabbit polyclonal 1:100-1:500	Sigma-Aldrich, HPA 030850, AB_10600764
Bassoon	Recombinant rat Bassoon	Mouse monoclonal 1:500	Life Science, SAP7F407, AB_10618753
Calbindin D-28K	Calbindin D-28K Chicken calbindin D-28K, full-length amino acid (aa) sequence	Mouse monoclonal 1:1,000	Sigma-Aldrich, C9848, AB_2314065
CHX10	amino acids 44–61 of human CHX10 (sequence PPSSHPRAALDGLAPGHL)	Goat polyclonal 1:100	Santa Cruz Biotechnology, sc-21690, AB_2216006
CtBP2	C-terminal binding protein-2 from mouse (361–445)	Mouse monoclonal, 1:10000	BD Bioscience, 612044, AB_399431
GAD67	Amino acid residues 4–101 of human GAD67	Mouse monoclonal 1:1000	EMD Millipore, MAB5406, AB_2278725
Glycine	Glycine paraformaldehyde-conjugated to thyroglobulin	Rat polyclonal 1:100	ImmunoSolution, IG1002, AB_10013222
Goα	Purified Goα from bovine brain	Mouse monoclonal 1:5000	EMD Millipore, MAB3073, AB_94671
Metabotropic glutamate receptor 6 (mGluR6)	AAPPQNENAEDAK, corresponding to the carboxy-terminus of rat mGluR6	Guinea pig 1:500	Neuromics, GP13105, AB_2341540
Peanut agglutinin (PNA)	No immunogen; binds to galactosyl (b-1,3) N-acetylgalactosamine, fluorescein labeled	300 µg/ml	Vector, FL-1071
Protein kinase C (PKC)	PKC (79–80 kDa) purified from bovine brain	Mouse monoclonal 1:1000	Biodesign International, K01107M, AB_2313750
PKC	purified bovine PKC, and its epitope mapped to its hinge region (amino acids 296–317)	Mouse monoclonal 1:100	Santa Cruz Biotechnology, sc-80, AB_628141
postsynaptic density protein	Recombinant rat PSD-95	Mouse monoclonal	EMD Millipore, MAB1596,

95 (PSD-95)		1:1000	AB_2092365
RNA Binding Protein Multiple Splice (RBPMS)	N-terminus of the RBPMS polypeptide ($RBPMS_{4-24}$), GGKAEKENTPSEANLQEEEVR	Guinea pig polyclonal 1:20000	PhosphoSolutions, 1832-RBPMS, AB_2395389
vesicular γ-aminobutyric acid transporter (VGAT)	Synthetic peptide AEPPVEGDIHYQR (amino acids 75–87 in rat) coupled to keyhole limpet hemocyanin via an added N- terminal cysteine.	Mouse monoclonal 1:1,000	Synaptic Systems, 131 011, AB_10890167
vesicular glutamate transporter 1 (VGluT1)	Amino acid residues 541-560 of rat vGLUT1	Guinea pig polyclonal 1:1000	EMD Millipore, AB5905, AB_2301751

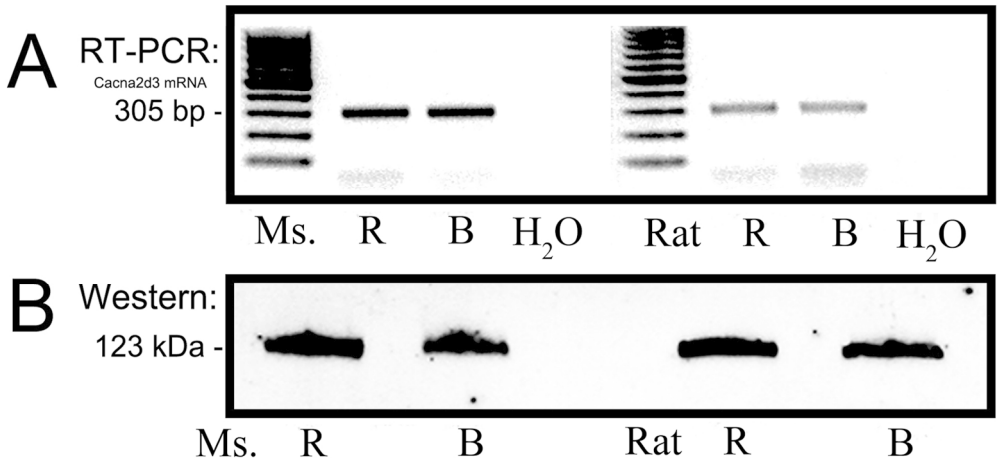

Figure 1. Expression of the voltage-gated accessory calcium channel α2δ3 subunit mRNA and protein in mouse and rat brain and retina extracts. (A) RT-PCR α2δ3 subunit primers in mouse and rat brain and retina extracts. (B) Western blots using the α2δ3 antibody in the mouse and rat retina and brain homogenates. A protein band of ~123 kDa was detected in these tissues. Ms=Mouse, R=Retina, B=Brain.
171x82mm (300 x 300 DPI)

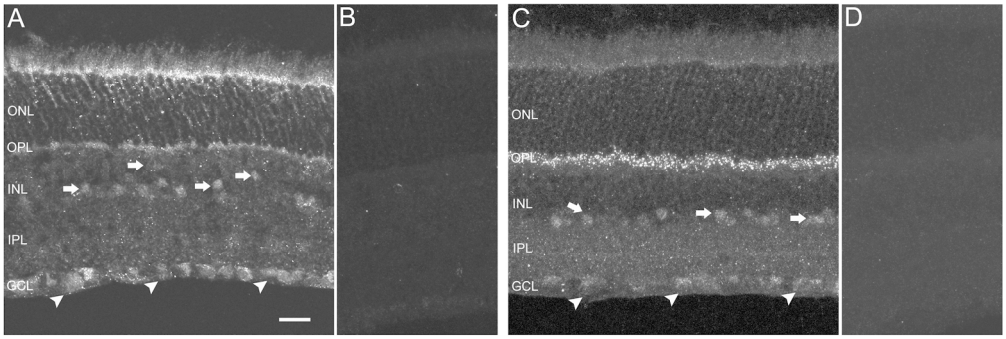

Figure 2. Localization of α2δ3 accesory calcium channel subunit immunoreactivity in the rodent retina. (A) Expression of α2δ3 subunit in the rat retina. α2δ3 immunostaining was in cells in the GCL (arrowheads), INL (arrows) and processes in the OPL. (B) No staining was observed in retinas incubated with antibodies preadsorbed with the immunization peptide. (C) Expression of α2δ3 subunit in the mouse retina. α2δ3 immunostaining was in cells in the GCL (arrowheads) and INL (arrows) and with strong immunoreactive puncta in the OPL. (D) No staining was observed in mouse section incubated with the blocking peptide as a control for the specificity of the antibody. ONL: outer nuclear layer; OPL: outer plexiform layer; INL: inner nuclear layer; IPL: inner plexiform layer; GCL: ganglion cell layer. Scale bars: 20 μm.
171x56mm (300 x 300 DPI)

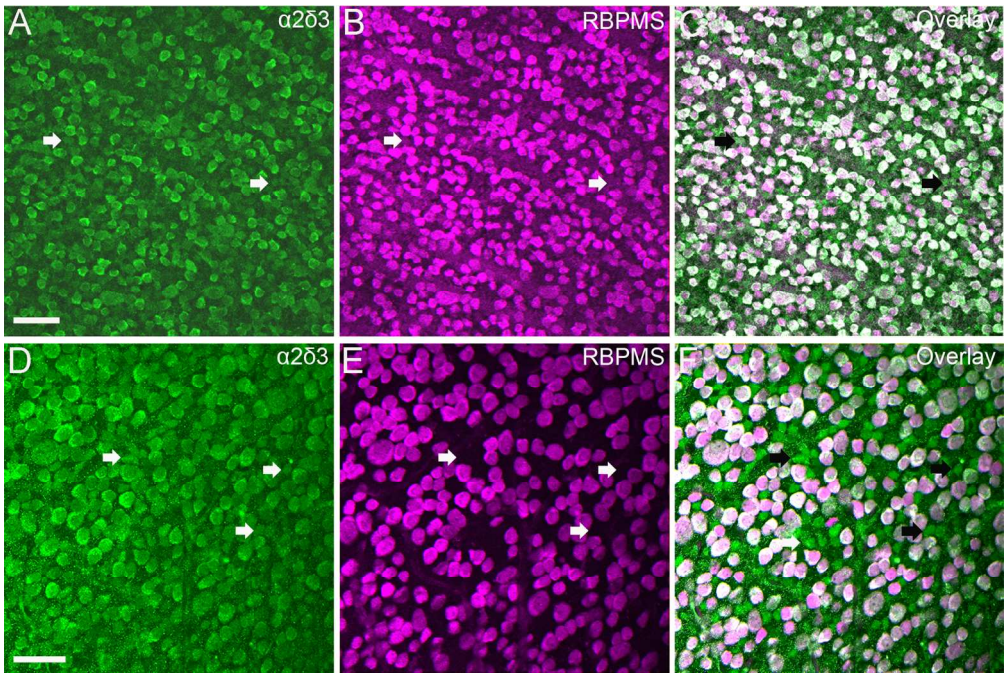

Figure 3: α2δ3 immunoreactivity (green) was expressed in RBPMS (magenta)-containing cells in the rat (A-C) and mouse (D-F) GCL. RBPMS is a selective marker for RGCs. Arrows indicate cells containing α2δ3 immunoreactivity and no RBPMS immunoreactivity, indicating that they are displaced amacrine cells. Scale bars: 50 μm.
171x114mm (300 x 300 DPI)

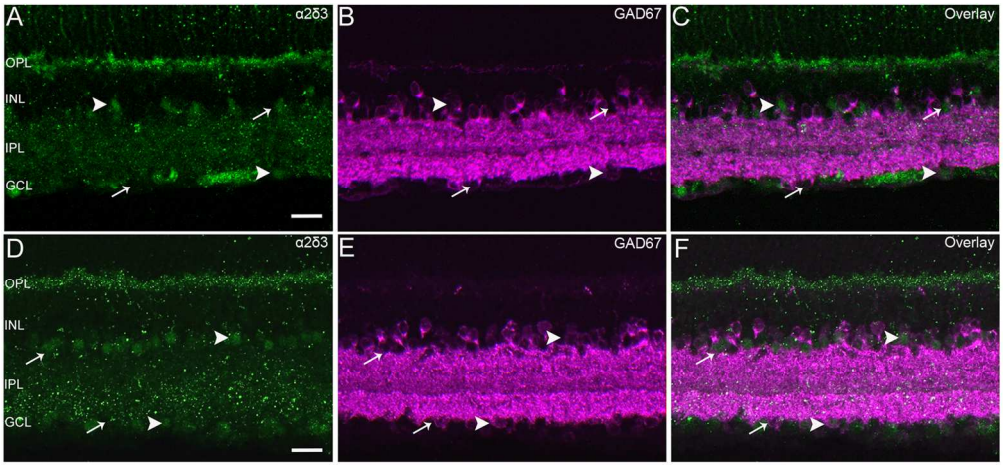

Figure 4: Localization of GAD67 and α2δ3 subunit immunoreactivities in the rodent retina. (A) α2δ3 immunostaining (green) in the rat retina. (B) GAD67 (magenta) immunolabeled IPL, OPL, and cell bodies in the proximal INL and GCL. (C) Merge image showing that some (arrowheads) but not all GAD67 (arrows) express the α2δ3 subunit in the GCL and INL. (D) α2δ3 immunostaining (green) in the mouse retina. (E) GAD67 (magenta) and (F) merge image showing colocalization of the α2δ3 subunit (arrowheads) with some but not all GAD67 amacrine cells (arrows) in the GCL and INL. OPL: outer plexiform layer; INL: inner nuclear layer; IPL: inner plexiform layer; GCL: ganglion cell layer. Scale bar (A-H): 20 μm.
171x78mm (300 x 300 DPI)

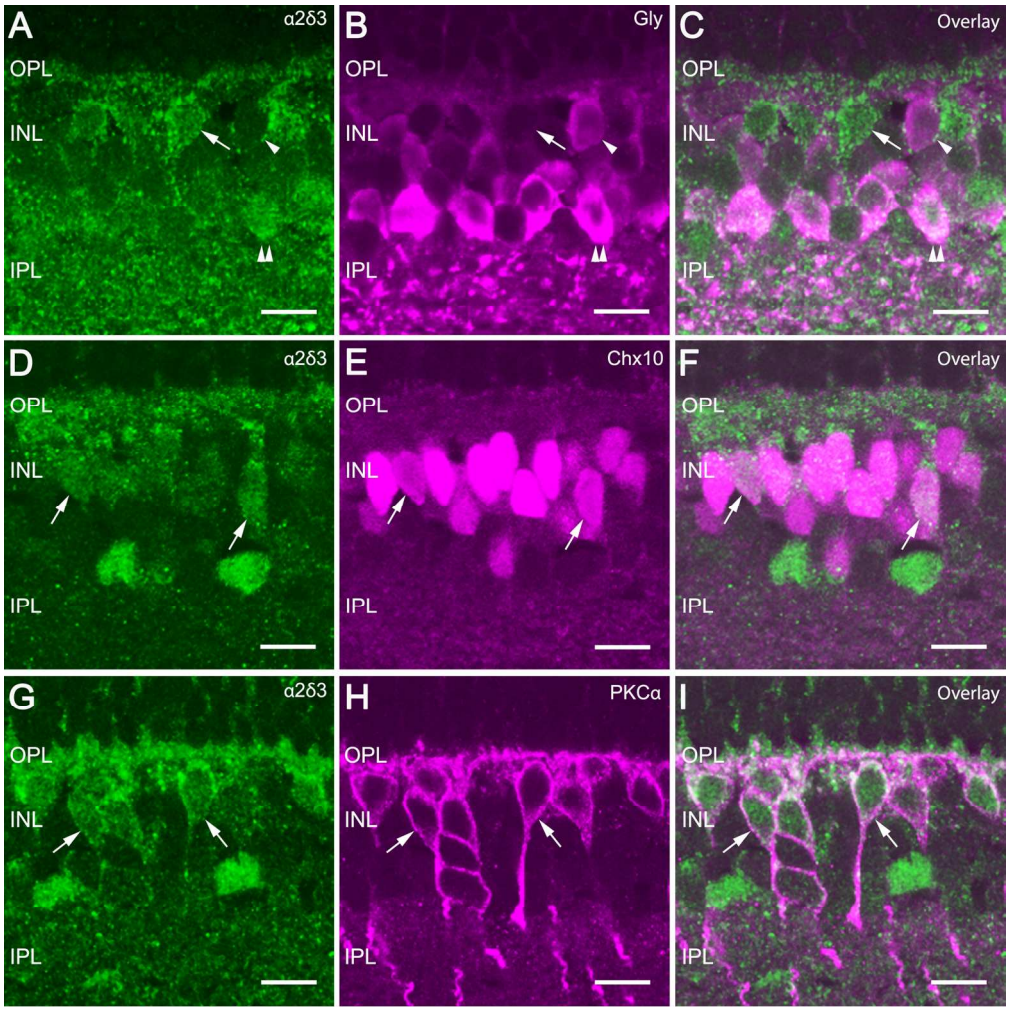

Figure 5: Localization of α2δ3 subunit in bipolar cells of the rat retina. (A) α2δ3 immunostaining (green) in the rat retina. (B) Immunostaining against glycine (magenta) stained bipolar cells through gap junctions with AII cells and revealed that some ON bipolar cells were immunostained by α2δ3 subunit antibodies (A-C, arrowheads) while other ON bipolar cells were not (arrows). Some glycinergic amacrine cells were positive for α2δ3 immunostaining (double arrowheads). (D) α2δ3 immunostaining (green) in the rat retina. (E) Chx10 (magenta), a pan-bipolar cell marker. (F) Colocalization of α2δ3 in some bipolar cells in the cell body (arrows). (G) α2δ3 immunostaining (green) in the rat retina. The immunostaining with PKCα antibody (magenta), a marker for rod bipolar cells (H), revealed co-localization with α2δ3 in rod bipolar cells (G-I, arrows). OPL: outer plexiform layer; INL: inner nuclear layer; IPL: inner plexiform layer. Scale bar: 10 μm.
171x171mm (300 x 300 DPI)

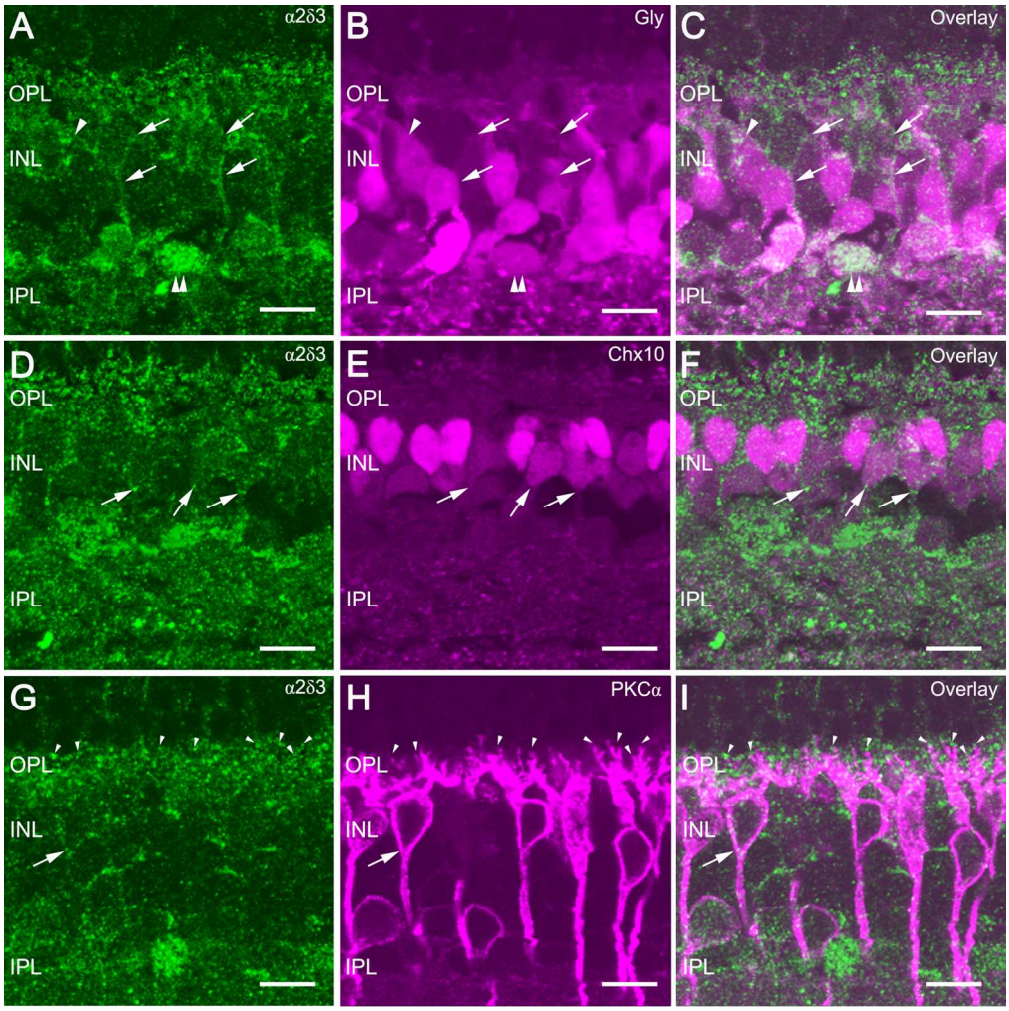

Figure 6
171x170mm (300 x 300 DPI)

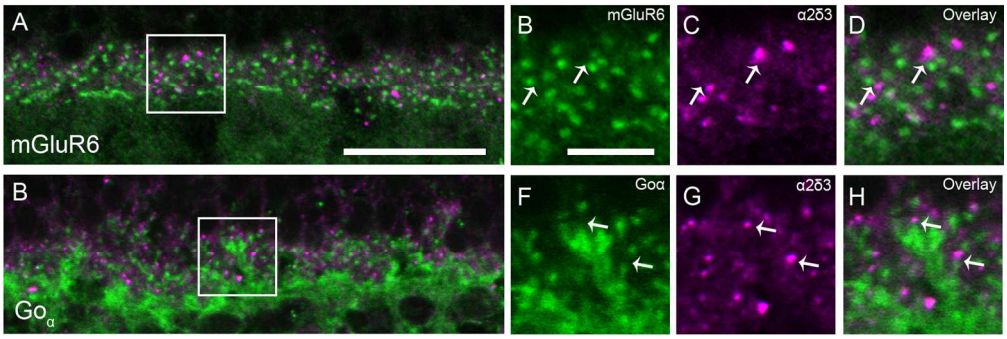

Figure 7. α2δ3 accessory calcium channel subunit is not in bipolar cell tips in the OPL of the mouse retina. (A) Double immunostaining of retinal sections with mGluR6 (green) and α2δ3 (magenta). (B-D) High magnification of single scan showing that mGluR6 immunoreactivity does not co-localize with the α2δ3 accessory calcium channel subunit (arrows). (E) Goα-immunoreactivity (green) and α2δ3-immunoreactivity subunit (magenta). (F-H) High-power photomicrograph image (boxed area from E) showing that Goα-immunoreactivity and α2δ3 subunit do not colocalized (arrows). Z-step = 0.33 µm. Scale bars (A, B): 20 µm, (B-D, F-H): 5 µm.
171x56mm (300 x 300 DPI)

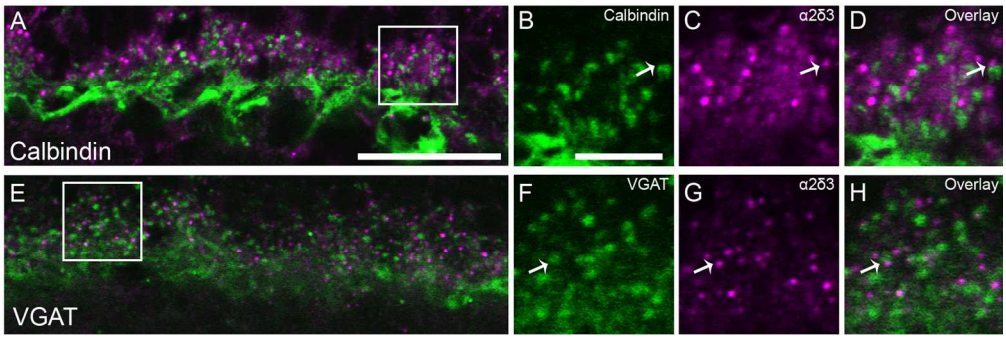

Figure 8. α2δ3 accessory calcium channel subunit is not expressed by horizontal cells in the mouse retina. (A) Single scan (boxed area from A) showing horizontal cells with calbindin and α2δ3 subunit staining (magenta). (B-D) High magnification of single scan showing α2δ3 subunit and horizontal cell processes. α2δ3 subunit was never found to be colocalized with horizontal cells or their processes. (E) Single scan showing horizontal cells tips labeled with a VGAT antibody (green) and α2δ3 subunit staining (magenta). (F-H) High magnification (boxed area from E) of single scan showing α2δ3 subunit staining. Z-step = 0.33 µm. Scale bar in (A, E): 20 µm, (B-D, F-H): 5 µm.
171x56mm (300 x 300 DPI)

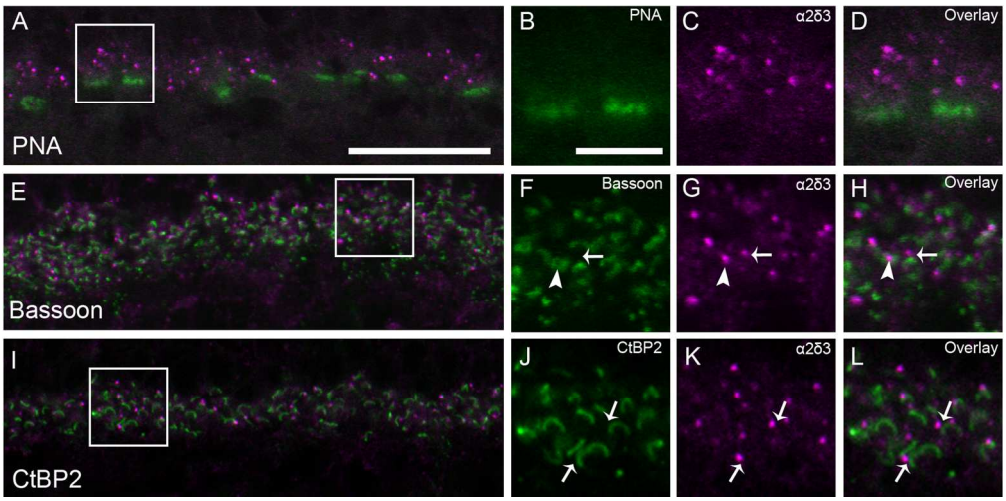

Figure 9. α2δ3 accessory calcium channel subunit in photoreceptors of the mouse retina. (A) Labeling of cone pedicles with PNA–FITC and α2δ3 accessory calcium channel subunit. (B-D) High magnification of single scan indicating that α2δ3 subunit is not located in the base of cone pedicles. (E) Double immunolabeling of α2δ3 accessory calcium channel subunits (magenta) and Bassoon (green), a presynaptic protein. (F-H) High magnification (boxed area from E) showing colocalization of some α2δ3 subunits (arrowheads). (I) Double immunolabeling of α2δ3 accessory calcium channel subunits (magenta) and CtBP2 (green), a ribbon synapse marker. (J-L) High magnification (boxed area from I) showing that a few of the α2δ3 subunits are adjacent to CtBP2 (arrows). Z-step = 0.33 µm. Scale bars (A, E, I): 20 µm; (B-D, F-H, J-L): 5 µm.
171x83mm (300 x 300 DPI)

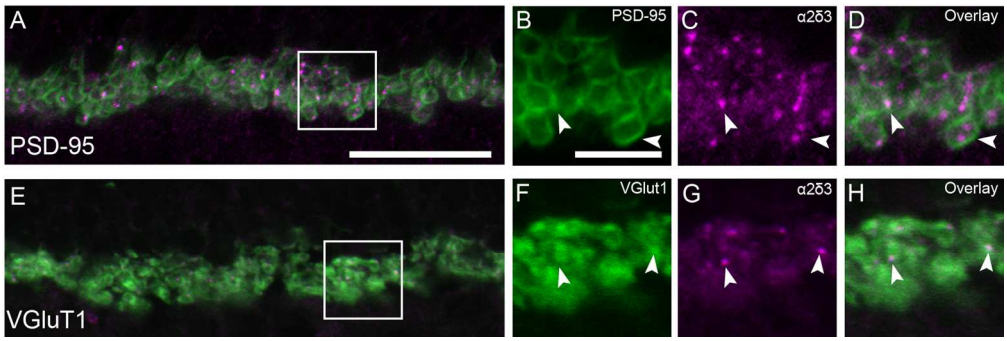

Figure 10. α2δ3 accessory calcium channel subunit in photoreceptors of the mouse retina. (A) Double immunolabeling of postsynaptic density protein 95 (PSD-95) (green) and α2δ3 subunit (magenta) in the mouse retina. (B-D): High-magnification view (boxed area from A) showing that all α2δ3 immunoreactive puncta were distributed inside the photoreceptor terminals. (E) Double immunolabeling of VGluT1 (green) for photoreceptor axon terminals and α2δ3 subunit (magenta) in the mouse retina. (F-H): High-magnification view (boxed area from E) showing that α2δ3 immunoreactive puncta are located inside the photoreceptor terminals. Z-step = 0.33 µm. Scale bars (A, E): 20 µm; (B-D, F-H): 5 µm.
171x56mm (300 x 300 DPI)

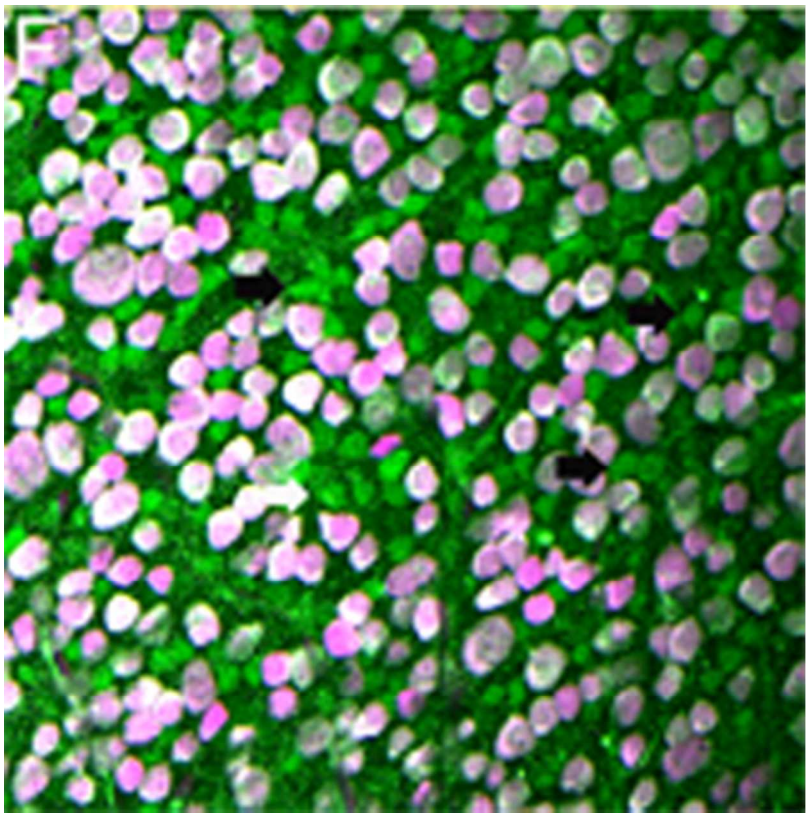

141x142mm (72 x 72 DPI)

Graphical abstract texct: $\alpha_2\delta_3$ immunoreactivity (green) was expressed in RBPMS (magenta)-containing cells in the mouse GCL. RBPMS is a selective marker for RGCs. Arrows indicate cells containing $\alpha_2\delta_3$ immunoreactivity and no RBPMS immunoreactivity, indicating that they are displaced amacrine cells.